15

Downloaded from http://portlandpress.com/biochem/jarticle-pdf/doi/10.1042/BCJ20253151/978745/bcj-2025-3151.pdf by University College London user on 14 October 2025

- 1 Phosphorus-specific, liquid chromatography inductively coupled plasma mass-spectrometry
- 2 for analysis of inositol phosphate and inositol pyrophosphate metabolism
- ¹Colleen Sprigg, ¹Hayley L. Whitfield, ¹Philip T. Leftwich, ²Hui-Fen Kuo, ²Tzyy-Jen Chiou, ³Adolfo
- 4 Saiardi, ⁴Megan L. Shipton, ⁴Andrew M. Riley, ⁴Barry V.L. Potter, ⁵Dawn Scholey, ⁵Emily Burton, ⁶Mike
- 5 R. Bedford, ¹Charles A. Brearley
- 6 ¹School of Biological Sciences, University of East Anglia, Norwich Research Park, Norwich NR4 7TJ, UK
- 7 ²Agricultural Biotechnology Research Center, Academia Sinica, Taipei 115, Taiwan
- 8 ³Laboratory for Molecular Cell Biology, University College London, London WC1E 6BT, UK
- 9 ⁴Medicinal Chemistry & Drug Discovery, Department of Pharmacology, University of Oxford,
- 10 Mansfield Road, Oxford OX1 3QT, UK
- ⁵School of Animal, Rural and Environmental Sciences, Nottingham Trent University, Southwell,
- 12 Nottingham NG25 0QF, UK
- ⁶AB Vista, Marlborough SN8 4AN, UK
- 16 Charles A. Brearley; orcid.org/0000-0001-6179-9109

Michael R. Bedford orcid.org/0000-0002-5308-4290

- 17 Emily Burton; orcid.org/0000-0003-2784-6922
- Tzyy-Jen Chiou; orcid.org/0000-0001-5953-4144
- 19 Hui-Fen Kuo; orcid.org/0000-0002-9169-3679
- 20 Philip T. Leftwich; orcid.org/0000-0001-9500-6592
- 21 Barry V.L. Potter; orcid.org/0000-0003-3255-9135
- 22 Andrew M. Riley; orcid.org/0000-0001-9003-3540
- 23 Adolfo Saiardi; orcid.org/0000-0002-4351-0081
- 24 Dawn Scholey; orcid.org/0000-0003-2450-5989
- 25 Megan L. Shipton; orcid.org/0000-0002-9982-0927
- 26 Colleen Sprigg; orcid.org/0000-0001-7755-4245
- 27 Hayley L. Whitfield; orcid.org/0000-0001-6003-7874
- 29 Abstract

28

- 30 Inositol phosphate (InsP) and diphosphoinositol phosphate (PP-InsP) analysis in tissues is plagued by
- 31 multiple difficulties of sensitivity, regioisomer resolution and the need for radiolabeling with
- 32 metabolic precursors. We describe a liquid chromatography (LC) inductively coupled plasma (ICP)
- 33 mass spectrometry (MS) method (LC-ICP-MS) that addresses all such issues and use LC-ICP-MS to
- 34 analyse InsPs in avian tissues. The highly sensitive technique tolerates complex matrices and, by

- powerful chromatography, resolves in a single run multiple non-enantiomeric myo-inositol
- 36 tetrakisphosphates, myo-inositol pentakisphosphates and all inositol hexakisphosphates, including
- 37 myo-inositol 1,2,3,4,5,6-hexakisphosphate (phytate), known in nature. It also separates and
- quantifies diphospho *myo*-inositol pentakisphosphate (PP-InsP₅) isomers from their biological
- 39 precursors and from 1,5-bis-diphospho myo-inositol 2,3,4,6 tetrakisphosphate (1,5-[PP]₂-InsP₄). Gut
- 40 tissue inositol phosphates, belonging to a non-canonical, lipid-independent pathway, are shown to
- 41 differ from phytate digestion products and to be responsive to diet.

43

Introduction

- 44 Inositol phosphates (InsPs) are canonical agents of intracellular signalling, with diverse cell biological
- 45 function (1-3). Of the 63 possible isomers of phosphate monoester-substituted myo-inositol,
- discrete function is assigned to a handful of species. Of these, inositol 1,2,3,4,5,6-hexakisphosphate,
- 47 InsP₆, phytate, is the most abundant InsP in the biosphere. Phosphorylation of its monoester
- 48 substituents gives rise to diphosphoinositol phosphates (PP-InsPs), the biological functions of which
- 49 are reviewed (4). Consequently, InsP₆ has a central position in flux of inositol between inositol
- 50 pentakisphosphate (InsP₅) and PP-InsP pools. It is important therefore that analysis of InsP
- 51 metabolism shows the relationship between InsP₅, InsP₆ and PP-InsP pools. Here, our understanding
- of the roles of InsP₆, PP-InsPs and other InsPs rests heavily on analysis of cell-lines. The behaviour of
- 53 these lacks tissue context.
- 54 Among InsPs, InsP₆ is a potent antinutrient of animals and human populations on subsistence diets
- and a significant risk factor in iron deficiency anaemia (5, 6). The enzymes that interconvert InsPs,
- 56 PP-InsPs and their inositol precursor have been found to participate in inflammatory responses (7-9)

- 57 and pathologies including cancer (10), diabetes (11), chronic kidney disease (12, 13), colitis (14) and
- 58 reproductive disorders (15), reviewed (1, 2, 4). Even so, despite numerous studies implicating InsPs
- and PP-InsPs in disease there have been remarkably few descriptions of the InsPs and PP-InsPs of
- 60 native tissues and organs and their response to therapeutic agents or environment including diet
- and metabolic insult.
- 62 The dearth of tissue analyses is in part due to the technical difficulty of measuring multiple
- stereoisomers at low concentrations. Radiolabelling of primary cells or tissue slices is an alternative
- 64 that has also been applied in cell lines, unicellular organisms, including algae, yeast and protists and
- 65 multicellular organisms, predominantly plants. The use of metabolic tracers, myo-[3H]-inositol or
- 66 [32P]-orthophosphate, bears the caveat of assumption of labelling to equilibrium. Alternatively, it is
- 67 inverted in non-equilibrium labelling studies that have defined pathways of synthesis of InsPs. Even
- so, radiolabelling is time consuming and comes with regulatory constraints.
- The opportunity to assign identity to and to measure InsPs and PP-InsPs without labelling has always
- 50 been recognized as an imperative even if not readily attainable. The metal-dye-detection (m-d-d)
- 71 HPLC method of Mayr (16) offers sensitivity at low pmol levels but sample work-up is involved and
- 72 time-consuming. Capillary electrophoresis mass spectrometry (CE-MS) offers fmol sensitivity at the
- cost of both time and concentration/pre-purification of InsPs and PP-InsPs on TiO₂ (17). A corollary is
- 74 that CE-MS is unsuitable for crude or complicated matrices. CE-MS further demands challenging
- organic syntheses of ¹³C standards (isotopologues) for calibration and for confirmation of identity of
- 76 peaks and has yet to be successfully adopted beyond the originating laboratory. Consequently, with
- 77 the explosion of interest in PP-InsPs (1, 2, 4), which constitute a tiny mole fraction of the total InsP

(and PP-InsP) content of tissues, there is a need for alternative approaches that can vouchsafe the intricacies of InsP and PP-InsP function without the constraints of radiolabelling or pre-purification.

An ability to handle complicated or crude matrices is desirable because these are information rich. InsPs and PP-InsPs are commonly extracted from animal cells and tissues with perchloric acid or trichloroacetic acid; from seeds, beans, and grains with hydrochloric acid; from animal gut contents or faecal matter with NaF-EDTA; and from soil matrices with NaOH-EDTA. From a chromatographic perspective, these extractants are generally considered not compatible with LC-MS or CE-MS, either because of the constraints of column chemistry or the extreme sensitivity of CE to ionic content. From a detection perspective, electrospray MS detection is susceptible to ion suppression effects. Consequently, both conventional LC-MS and CE-MS demand exchange of extractant for more benign loading solutions. The much higher sample loading available on anion-exchange LC (hundreds of

Herein, we elaborate on how liquid chromatography inductively-coupled-plasma-mass spectrometry (LC-ICP-MS) allows measurement of InsPs and PP-InsPs in crude or purified biological matrices across taxa. The interpretation of chromatography is remarkably simple, as is the nature of detection: detector response is proportional to phosphorus content, and the detector signal does not require complicated de-convolution.

microliters) compared to CE (a few nanoliter) is a potential advantage of the former method.

Results

80

81

82

83

84

85

86 87

88

89

90

91

92

93

94

95

96

97

98

99

100

101

102

103

104

105

106

107

108

109

110

111

112

113

114

115

116117

118

119120

121

Chromatographic resolution of multiple InsP₄, InsP₅, InsP₆ and PP-InsP isomers on a single gradient.

Downloaded from http://portlandpress.com/biochemi/article-pdf/doi/10.1042/BCJ20253151/978745/bcj-2025-3151.pdf by University College London user on 14 October 2025

ICP-MS is a powerful approach for elemental analysis but is rarely coupled to liquid chromatography (18). In contrast, MS and tandem MS-MS is commonly coupled to liquid chromatography in pharmaceutical and biomedical contexts, while CE-MS use is much less common across disciplines. The example taxa/matrices analysed in this manuscript are shown (Figure 1A). Each demands different extraction regimes. The different InsPs and PP-InsPs contained therein can be analysed by a single chromatographic approach (LC) coupled to phosphorus-specific detection (ICP-MS) and can all be placed within generic pathways of higher InsP and PP-InsP synthesis, whether derived from lipid or 'soluble' precursors (Figure 1B). The structures and enantiomeric relationships of all myo-InsP₅, InsP₆ and PP-InsP₅ isomers are shown (Figure 1C). Separation of InsPs and PP-InsPs bearing between two and eight phosphates is possible in a single chromatographic run with detection of the phosphorus content by ICP-MS (Figure 1D). Like CE-MS (17), LC-ICP-MS identifies 1/3-PP-InsP₅, 4/6-PP-InsP₅, 5-PP-InsP₅, 1,5-[PP]₂-InsP₄ and 4/6,5-[PP]₂-InsP₄ in *Dictyostelium discoideum* (Figure 2) but simultaneously measures multiple InsP₄ species and all InsP₅ species. We note resolution of a minor peak eluting shortly after InsP6 at approximately 26 min that is most likely an endogenous PP-InsP4, of unknown regiochemistry. Without chiral stationary phases or chiral shift reagents, neither CE-MS nor LC-ICP-MS resolve enantiomers, viz. 1-PP-InsP₅ and 3-PP-InsP₅ or 4-PP-InsP₅ and 6-PP-InsP₅ named with 1/3- and 4/6- prefixes in the preceding sentence. Similarly, it is not possible to resolve $Ins(2,3,4,5,6)P_5$, hereafter $InsP_5$ [1-OH], from $Ins(1,2,4,5,6)P_5$, hereafter $InsP_5$ [3-OH], or $Ins(1,2,3,5,6)P_5$, hereafter $InsP_5$ [4-OH], from $Ins(1,2,3,4,5)P_5$, hereafter $InsP_5$ [6-OH]. We use the term $InsP_5$ [1/3-OH] and $InsP_5$ [4/6-OH] where the speciation of enantiomers is unknown.

Among biological matrices, soils are unique in the breadth of inositol hexakisphosphate species present A direct comparison of LC-ICP-MS and ³¹P NMR for analysis of inositol phosphates in a Swedish podsoil was made (19), with detector response for phosphorus differing by less than 7% across the HPLC gradient. Here we show how a short, steeper linear gradient of HCl also resolves all

known naturally occurring inositol hexakisphosphates, neo-InsP₆, D-chiro-InsP₆, myo-InsP₆ and scyllo-

- 123 InsP₆, present in a Chernozem soil sample, in addition to both *neo*-InsP₅ and *scyllo*-InsP₅ (Figure 3).
- 124 Chromatograms for dilutions of an InsP₆ hydrolysate or InsP₆ standard are shown (Figure 3B, C). A
- calibration curve for detection of phosphorus (phosphate) is shown (Figure 3D).

126

127

- LC-ICP-MS identifies InsPs in complicated matrices without pre-purification of analytes
- 128 CE-MS of InsPs in mammalian tissues, cell lines, mouse tissues, plants, amoebae, and yeast is
- dependent on extraction with HClO₄ and pre-purification on TiO₂ (17). Analysis of crude extracts
- offers complementary information, as in description of dietary influence on InsPs of the gut lumen of
- chicken where simple NaF-EDTA extraction at alkaline pH is common (20, 21). Here we treat the gut
- lumen as an organ, a concept widely accepted in modern microbiome health contexts (22).
- 133 Accordingly, we first analysed InsPs in NaF-EDTA extracts of gastro-intestinal contents (digesta) of
- 134 gizzard and ileum of birds fed two levels of phytase in their diet. InsP₂ (isomers unidentified), InsP₃
- 135 (isomers unidentified), Ins(1,2,3,4)P₄, Ins(1,2,4,5)P₄, Ins(2,3,4,5)P₄, Ins(1,4,5,6)P₄, InsP₅ [5-OH], InsP₅
- [4/6-OH], InsP₅ [1/3-OH] and InsP₆ were detected in digesta of birds fed the lower (500 FTU/kg) dose
- of phytase by LC-ICP-MS (Figure 4, Figure S1A,B). At 6000 FTU/kg, inositol phosphates were barely
- detectable, having been fully degraded.
- 139 For comparison with established methodology, gizzard lumenal samples were also analysed by HPLC-
- 140 UV (Figure S1C). This method reports on analytes that interact with ferric ion. While these include
- InsPs, and PP-InsPs (23, 24), other analytes that chelate or engage in Fenton chemistry with ferric ion

- in the acid conditions of the chromatography will interfere. These potentially include catechols,
- diarylcyclopentenones and flavonoids. As these molecules lack phosphorus, they do not interfere
- with LC-ICP-MS. For comparison, the LC-ICP-MS data (Figure S1A,B) were obtained from 10 μL of a
- 145 10-fold diluted NaF-EDTA extract while the HPLC-UV data (Figure S1C) were obtained from 20 µL of
- the undiluted NaF-EDTA extract. LC-ICP-MS is approximately 2 orders of magnitude more sensitive.
- Ins(2,3,4,5)P₄ is the predominant InsP in both the ileal and gizzard digesta analyzed (Figure 4, Figure
- 148 S1).
- 149 The 6-phytase used in this feeding trial is a modified *E. coli*-derived enzyme. The first
- characterization of this enzyme was reported (25). The principal pathway of dephosphorylation of
- phytate in the chicken digestive tract is shown (Figure S1D), after (20, 21). It is characterized by
- retention of the axial 2- phosphate at all levels of dephosphorylation as far as InsP. Because the birds
- were fed a mash diet, not heat-treated, additional endogenous phytase activity of the wheat-based
- diet (which possesses very high mature grain phytase activity (26)) is apparent in the generation of
- InsP₅ [5-OH] in the gizzard lumen (Figure S1A-C). InsP₅ [5-OH] is a characteristic product of Triticeae
- 156 (cereal, including wheat) purple acid phytase (27). The effect of dietary treatment on lumenal InsP
- content of gizzard and ileum was published previously (28). Digestion of dietary InsP₆ liberates
- inositol, which passes by undefined mechanism to the blood. Inositol levels of jejunum tissue,
- 159 kidney and blood correlate positively with lumenal inositol content of the jejunum (29). Similarly,
- ileal lumen (digesta) inositol correlates positively with blood inositol (21). These analyses highlight
- how digestion releases the inositol precursor of tissue InsP and PP-InsP synthesis into the blood.
- 162 InsPs of duodenum, jejunum and ileum tissues can be analysed by LC-ICP-MS.
- 163 Gut tissues are bounded on one side by the lumen and on the other by the bloodstream. The blood
- receives nutrients from the gut (Figure 5A). The hepatic portal vein drains blood from the
- gastrointestinal tract to the liver. The predominant cells of the blood are erythrocytes. Avian blood

shares the same inositol phosphate species as the duodenum, jejunum and ileum (Figure 5B-D, Figure S2) but lacks appreciable InsP₆, which is a substantial component of duodenum, jejunum and ileum tissue InsPs. The blood InsP profile is consistent with m-d-d HPLC, NMR and radiolabelling (16, 30, 31), the latter revealed that the specific enantiomer Ins(3,4,5)P₃ is the precursor of the specific enantiomer Ins(3,4,5,6)P₄ and the latter is the precursor of Ins(1,3,4,5,6)P₅, InsP₅ [2-OH] (30). We may assume that InsP₅ 2-kinase catalyzes the final step of InsP₆ synthesis as described for other animals, plants and yeast (32). The liver, distal to the gut, and the kidney share the same major species Ins(3,4,5,6)P₄ and InsP₅ [2-OH], again with lower levels of InsP₆ (Figure 5D and (28)). InsP₅ [2-OH] is not a product of known phytases (33), including multiple inositol polyphosphate phosphatase, MINPP (34, 35). Because the other InsP₅ species are only minor components of these tissues, the data shown (Figure 5) make it likely that a common 'soluble' pathway/network of InsP₆ synthesis, Ins(3,4,6)P₃ to Ins(3,4,5,6)P₄ to Ins(1,3,4,5,6)P₅ to Ins(1,2,3,4,5,6)P₆ that is discrete from the lipid-derived pathway that contributes Ins(1,4,5)P₃ to cytosolic InsP metabolism (32), is operative organ wide in avians. Moreover, the absence of the 2-phosphate distinguishes intermediates of synthesis (Figure 5E) from lumenal digestion (Figure S1D).

While myo-inositol is the scaffold on which our understanding of biological function of inositol phosphates is built in mammals, avians, fungi and plants, myo-inositol hexakisphosphate (InsP₆) is not the only naturally biological isomer: apart from its presence with other isomers in soil (19, 36), neo-inositol hexakisphosphate (neo-InsP₆) is found in $Entamoeba\ histolytica$ (37). Use of LC-ICP-MS discounts the presence of D-chiro-, neo and scyllo-inositol hexakisphosphates in the avian tissues/organs analysed. This issue has not, to our understanding, been tested formally elsewhere.

Downloaded from http://portlandpress.com/biochemi/article-pdf/doi/10.1042/BCJ20253151/978745/bcj-2025-3151.pdf by University College London user on 14 October 2025

InsPs of duodenum, jejunum and ileum tissue are responsive to diet

A central theme of gut microbiome research is that the gut epithelium is responsive to factors generated in the gut lumen. While there are remarkably few studies of phytate digestion in rodent models, let alone humans, it was shown recently that oral gavage of mice, whose microbiota had been denuded by antibiotic treatment, with phytase producing microorganisms resulted in digestion of gavaged phytate, $InsP_6$ (38). Other than a recent report of application of CE-MS to mouse tissues including the colon and a single human biopsy thereof (39), and measurements of InsP₆ and unspecified PP-InsPs by HILIC-MS/MS (40, 41), we are not aware of detailed speciation of InsPs in gut tissues. Consequently, it is not known whether digestion of phytate has direct influence on gut InsP signalling, or on broader mammalian physiology beyond mineral deficiency (5, 6). In contrast, for avian species numerous feeding trials testing the effect of phytase treatment on InsP₆ digestion and animal performance have been reported (reviewed 42). They underpin practice in a food sector that raises c. 70 billion chickens per annum. Nevertheless, the effect of InsP₆ digestion on gut tissue inositol phosphates is undefined in any organism. Previously, by ad libitum feeding of diets supplemented or not with phytase, we showed that inositol phosphate metabolism of kidney tissue of broiler chickens is responsive to diet, to the interaction of inositol and phosphate released in the gut (28). Remarkably, this premise has not been tested in other species but must mechanistically involve direct influence of diet on gut tissue, because gut tissues are the conduit by which digestion products enter the circulatory system.

To test whether gut tissue signalling molecules, InsPs, are responsive to diet, we performed an animal feeding trial. The absence of detectable PP-InsPs in the tissue samples analysed in Figure 5 allowed use of the less-sensitive but more accessible HPLC-UV method (23). We note that the level of InsP₆ measured in chicken gut tissues for control diet-fed animals, 15-20 nmol/g wet weight, is comparable to that measured c. 70, nmol/g in mouse colon (39), and both are 2.5-10-fold less than reported by HILIC-MS/MS (41). For mice, the authors suggested that PP-InsPs of gut tissues may

224

225

226

227

228

229

230

231

232

233

234

235

236

237

238

239

240

241 242

243

244

245

246

212 have arisen from uptake from the gut lumen, i.e., been present in feed which was autoclaved. For 213 our study we have described the active phytase activity of the mash diet. It is possible therefore that 214 the absence of PP-InsPs in chicken gut tissues may reflect their digestion by feed and adjunct 215 phytases. Again, we know of no other measurement for this tissue/organ. The data presented in 216 Figure 6 represents analysis of c. 300 perchloric acid-extracted, and TiO₂-purified, tissue samples. For 217 each dietary treatment: control, 2g/kg inositol, 500 or 6000 FTU phytase/kg, all with or without 218 titanium dioxide, an inert marker of digestion, samples of tissue were taken from the duodenum, 219 jejunum, and ileum of twenty-four randomly selected individual birds (from a population of 480) and 220 analysed by HPLC. The feeding trial design was reported (43). Figure 6 shows the levels of InsP₃,

221 InsP₄, InsP₅ and InsP₆ measured, beside estimates of the mean and standard deviation generated by

222 a linear mixed model of data set.

> The data presented in Table S1 show the differences between the mean slopes, their confidence intervals, and the probabilities, referenced to the InsP₃ value of duodenal tissue samples taken from birds fed a control diet lacking titanium dioxide. Post hoc analysis of the global data set, i.e., without stratification, shows that gut tissue inositol phosphates were responsive to diet. The model predicts 75% of the variance across the entire data set. The jejunum showed a significant differential in response to the highest phytase levels between mean InsP levels (LMM Post hoc: Control - Phytase 6000 FTU/kg t_{2270} = -4.659 (nmol / g w wt), p < 0.001). Ileum tissue showed a significantly differential increase in InsP to inositol (LMM Post hoc: Control - Inositol $t_{227} = 5.593$, p < 0.001) and a marginally significant decrease in InsP to phytase (LMM Post hoc: Control - Phytase 6000 FTU/kg t_{227} = 3.267, p= 0.007. By individual InsPs there were no differential responses in InsP₃, InsP₄ or InsP₅ to phytase levels (p > 0.05) for any gut tissue, except for a marginally significant response for InsP₅ in jejenum (LMM Post hoc: Control - Phytase 6000 FTU/kg: t227 = 3.6, p = 0.002). All gut tissues showed a significant change in InsP₆ levels with the highest phytase levels (LMM Post hoc: Control - Phytase 6000 FTU/kg; duodenum t_{227} = 6.59, p <0.001, ileum t_{3227} = 8.04, p <0.001, jejenum t_{227} = 9.16, p<0.001).

Downloaded from http://portlandpress.com/biochemi/article-pdf/doi/10.1042/BCJ20253151/978745/bcj-2025-3151.pdf by University College London user on 14 October 2025

Because of the central role of InsP₆ in higher InsP and PP-InsP synthesis and the singular route of InsP₆ synthesis, from InsP₅ [2-OH] ³², we tested for effect of diet on InsP₅: InsP₆ ratio. Significant difference in InsP₅ [2-OH]: InsP₆ ratio was also detected between Control and Phytase 6000 groups for duodenum ($t_{18.3} = -3.2$, p = 0.002) and jejunum ($t_{19} = -4.7$, p < 0.001), but not for the ileum ($t_{18.4} = -4.7$), p < 0.0012.357, p = 0.12) (Table S2). These data highlight how important signalling molecules of tissue of the gut - lumen interface, InsP₅ [2-OH] and InsP₆, are manipulable by diet with dietary effects likely targeting InsP₅ 2-kinase. This enzyme is strongly reversible (44). The results of these studies illustrate the utility of LC-UV and LC-ICP-MS for inositol phosphate analysis and particularly for gutmicrobiome research. The data is also presented in Tables S3, S4 and S5.

247

248

249

250

251

252

253

254

255

256

LC-ICP-MS analysis of plant tissue

Phosphate is a major nutrient that limits plant growth. The mechanisms by which plants sense changing phosphate status of their tissue is intensely studied with predominant roles in the Phosphate Starvation Response identified for inositol phosphate kinases of the ITPK (45), IPK1 (IP₅ 2-K) (46, 47) and VIP (VIH) families (48), reviewed (49). These garner interest beside transporters that integrate whole plant response to phosphate availability (50). Replicate extractions of soil-grown ColO and pho2-1 (51) plants are shown (Figure 7). The latter shoot phosphate hyper-accumulation mutant which bears mutation in the UBC24 gene (52) shows levels of InsP₆ approximately double that of wild-type Col0, but without substantive change in overall inositol phosphate profile. ipk1,

extensively characterized in terms of inositol phosphate profile and phosphate hyper-accumulation, shows elevations in $Ins(3,4,5,6)P_4$ and $InsP_5$ [2-OH] as well as substantial reduction in $InsP_6$, whether measured by radiolabelling (45, 47, 53), CE-MS (53), or illustrated here for a single sample by LC-ICP-MS (Figure 7). The ABC transporter mutant mrp5 (54) also shows reduced seed $InsP_6$ and levels of InsPs like wild type in vegetative tissues (54, 55), shown here for a single sample (Figure 7).

262

263

264265

266267

268

269

270

271

272

273

274

275

276

277

278

279

280

281

282

283

284

285

286

287

288

289

290

291

292

293

294

295

296

297

298

299

300

301

Discussion

Considering the contribution of InsPs and PP-InsPs to cellular processes, including phosphate homeostasis and energy status (3, 46-49, 55), we thought that it might be useful to construct a technique, with capability of measuring phosphorus content of multiple isomers of InsPs and PP-InsPs alike. The value of the measurement of other inositol phosphates that are the metabolic precursors of InsP $_5$ species, InsP $_6$ and PP-InsPs, besides PP-InsPs themselves, is obvious, not least because 'small' changes may be overlooked, certainly where PP-InsPs are normalized to InsP $_6$, or where canonical pathways are assumed. More generally, without adoption of methods that cover the widest spectrum of InsPs, from InsP $_1$ to InsP $_6$ and PP-InsPs, and that can distinguish species unique to different pathways, the pleiotropic effects of disruption of individual genes on broadest InsP metabolism is likely hidden – particularly, where analysis is restricted to PP-InsPs.

By demonstrating the utility of LC-ICP-MS to handle diverse extractants, we show how the approach is relevant to InsP measurement in environmental samples and across taxa - here in Dictyostelium, plants and animals – and most obviously in context of animal nutrition and phosphate homeostasis. For the latter, we have shown how LC-ICP-MS is suitable for study of InsPs in animal physiological contexts. The differences in InsPs of the gut lumen and gut tissues constitute transmembrane gradients of important bioactive species. While the extent of vectorial transport of native InsPs across gut epithelia has not been described but has been suggested for PP-InsPs in mice (39), exchange of the contents of extracellular vesicles of the gut microbiome, particularly of Gram negatives such as Bacteroidetes, with gut epithelia is an emergent field (34, 56). Less ambiguously, InsP₆ is transported subcellularly by the ABC transporter MRP5 (ABCC5) (54). The presence of extracellular InsPs in kidney stones (57) and in the laminal layers of hydatid cysts of the Echinococcus granulosus (58) further evidence InsP transport widely across metazoan taxa. We reveal common synthesis/metabolism of InsPs in duodenum, jejunum, ileum, erythrocyte, and kidney of broiler chickens by a non-canonical pathway that is not obviously/directly related to phosphatidylinositol phosphate turnover (30, 32) and which, though isomerically distinct from digestion of dietary $InsP_6$ is demonstrably connected thereto. We show pronounced effect of diet on this non-canonical pathway in tissue of the duodenum, jejunum, and ileum, as well as effect on kidney (28). Put simply, inositol phosphate signalling molecules are shown to be responsive to diet at an interface, the gut, that has become the focus of human health research. Indeed, these tissues have a major role in immunity (59, 60) as well as digestion.

Downloaded from http://portlandpress.com/biochem/jarticle-pdf/doi/10.1042/BCJ20253151/978745/bcj-2025-3151.pdf by University College London user on 14 October 2025

In model systems, the effect of disruption of inositol phosphate multikinase (IPMK) has pleiotropic effects. These are attributed to InsPs and PP-InsPs (8, 61) and include influence on intestinal function (14, 62). Interestingly, disruption of IP6K2 was shown to alter PP-InsP $_5$ in rodent knock-out models, largely without effect on InsP $_6$. The levels of InsP $_6$, and consequently PP-InsP $_5$, in mouse gut tissues: stomach, small intestine, duodenum and colon, measured by HILIC MS (40) were considerably higher (e.g., approaching 600 and 22 pmol per mg, respectively, for small intestine) than in other tissues (41). The study did not describe isomers, other than InsP $_6$, but showed that purification of the diet which removed approximately 94% of InsP $_6$ and PP-InsP $_5$, altered gut tissue InsP $_6$ and PP-InsP $_5$ levels.

provided a reaction cell for reaction with oxygen, generating a PO+ ion m/z 47+ that was filtered in

the third quadrupole. The detector's dwell time was set to 50 msec or 500 msec, giving up to 45000

Downloaded from http://portlandpress.com/biochem/jarticle-pdf/doi/10.1042/BCJ20253151/978745/bcj-2025-3151.pdf by University College London user on 14 October 2025

339

340

341

data points for a 45-minute run.

343	HPLC-UV
344	Samples, 50 μL for tissue, were injected from a 200 μL loop of a Jasco (Japan) LC-4000 HPLC system
345	comprised of a AS-4195 autosampler, a Jasco PU-4185 gradient pump and a UV-4075 detector set at
346	290 nm. As for LC-ICP-MS, InsPs were resolved on a 3 mm x 250 mm Dionex CarboPac PA200 column,
347	fitted with 3 mm x 50 mm guard column. The column was eluted with either HCl or methanesulfonic
348	acid at a flow rate of 0.4 mL.min ⁻¹ . The column eluate was mixed with 0.1% w/v Fe(NO ₃) ₃ .9H ₂ O in 2%
349	w/w HClO ₄ (66). This was delivered post-column into a mixing Tee and from there to a 190 μL
350	volume, 0.25mm internal diameter reaction coil (delivered by a Jasco PU-4085 pump at a flow rate
351	of 0.2 mL min ⁻¹) before passage to the UV detector. Linear gradients of solvents: A (water) or B (HCl
352	or methanesulfonic acid) were mixed according to the following schedule: time, min; % B; 0, 0; 25,
353	100; 38, 100; 39, 0; 40, 0. Identification of inositol phosphates was made by comparison to a
354	reference sample of InsPs prepared by acid-hydrolysis of InsP ₆ (67). Concentration of InsPs was
355	established by reference to UV detector response to injection of InsP ₆ (23). Example coefficients of
356	variation for retention time of $Ins(3,4,5,6)P_4$, $Ins(1,3,4,5,6)P_5$ and $InsP_6$, with mean retention times:
357	19.37, 26.37 and 33.66 min, respectively, were 1.008, 0.959 and 1.133% for a set of 72 ileal tissue
358	samples run with standards over a period of 3d.
359	Data processing
360	LC-ICP-MS data were exported from Chromeleon software as x,y data (.csv) and imported into Jasco
361	ChromNav v.2 software for peak integration. For graphical presentation of chromatograms, x,y data
362	was imported into and plotted in ggplot2 after smoothing with a Savitzky–Golay filter with window
363	length of 11 and polynomial order of 2.
364	LC data generated during measurement of InsPs by post-column addition of ferric nitrate was
365	exported from Jasco ChromNav v.2 software as x,y data (.csv) (24). Data was imported into and
366	plotted in ggplot2 without smoothing or mathematical manipulation.
367	Statistical analysis
368	For the animal feeding trial, the results of which are shown in Figures 3 and 4, all analyses were
369	carried out in R ver 4.3.1. (68), with input the InsP content of tissues calculated from the integrated
370	HPLC-UV traces, examples of which are shown for digesta in Figure 3. Linear mixed-effects models
371	(LMM) were fitted with the ImerTest package (69), summarised with emmeans (70) and model
372	residuals were checked for violations of assumptions with the DHARMa package (71). Figures were
373	generated with ggplot2. Data analyses are briefly summarised below.
374	For individual InsP values we fitted a linear mixed model on log-transformed values with a constant
375	(1) added to each value, with diet (control, inositol added and two levels of phytase
376	supplementation), InsP type, titanium addition and tissue type as fixed effects, and two-way
377	interactions between InsP type, tissue and diet, the model also included individual and dietary pen
378	as random effects. When comparing the InsP ₅ : InsP ₆ ratio we modelled a square root transformation
379	of the ratios with diet, tissue type and titanium addition included as fixed effects, with an interaction
380	between diet and tissue type and individual included as random effect. The model also included
381	individual and dietary pen as random effects.
382	All linear mixed-effect models were fitted with REML and the nloptwrap optimiser for model
383	convergence. Where appropriate degrees of freedom were estimated with Satterthwaite's

approximation. Posthoc pairwise comparisons were carried out with the emmeans package and a

Tukey adjustment for multiple comparisons.

- 386 Animal Study: Diets, Animals and Management, Ethical Approval
- 387 The study was undertaken at the Poultry Research Unit, School of Animal, Rural and Environmental
- 388 Sciences, Nottingham Trent University (NTU) with ethical approval obtained from the NTU animal
- 389 ethics review committee (internal code ARE20213). UK national NC3R ARRIVE guidelines for the care,
- 390 use and reporting of animals in research were followed. Birds had ad libitum access to feed and
- water throughout the study.
- 392 Animals, Diet and Experimental Design
- 393 Birds, 480 male Ross 308 hatchlings, obtained from a commercial hatchery (PD Hook, Cote, Oxford,
- 394 UK) were allocated randomly to 48 floor pens on day 1. Animals were divided among 8 treatment
- 395 (diet) groups (Table S6). Of these diets, half were supplemented with 5 g/kg TiO₂ (Titanium, Ti, a
- 396 common inert marker of digestion) and the other half were not. With/without Ti, diets were
- labelled as Control (no further supplementation), Ins (supplemented with 2 g/kg 12 C/ 13 C inositol,
- containing ¹³C inositol at d30‰), or Phy500 or Phy600 (supplemented with 500 or 6000 FTU/kg
- 399 phytase). The phytase used was Quantum Blue and was supplied by AB Vista (Marlborough, UK). The
- composition of the basal diet, see (43), was formulated to according to the Ross Management
- 401 Manual 2018. 10 birds were allocated to 6 replicate pens for each treatment group with birds fed
- 402 the respective diets throughout the trial (1 to 21 days). A power calculation was made using data for
- response of mean gizzard and ileal inositol contents to phytase addition (72), indicating that 6
- replicates per treatment were sufficient to identify treatment differences at a power setting of 80%
- and a type 1 error rate of 5%.
- 406 Sampling
- Birds, 2 per pen, were selected at random and euthanised on d 21 post-hatch by cervical dislocation

- 408 without prior stunning in accordance with the Welfare of Animals at the Time of Killing (England)
- 409 Regulations (2015) guidelines for poultry. For each bird, the gizzard was excised, opened and the
- 410 contents scraped into a container as a pooled sample from both birds. Ileal digesta were collected
- 411 from the same two birds by gentle digital pressure, pooled and stored at -20°C prior to lyophilization.
- 412 They were subsequently freeze dried at -50°C for 7 days or until constant weight. Once dried,
- samples were finely ground using a coffee grinder and stored at 4°C until analysis.
- 414 From each of the two birds from which digesta was pooled for analysis, duodenum, jejunum and
- ileum samples were excised, taking care to ensure tissue was consistently excised from the same
- 416 region of organ for each bird. Samples were immediately frozen at -20°C before shipping to UEA and
- 417 thereafter were stored at -80°C. After defrosting, 100 mg slices of tissue were taken for InsP
- 418 extraction and analysis.
- 419 Analysis of inositol phosphates in digesta
- Diets, gizzard and ileal digesta were extracted as described [43]. In brief, 100 mg samples of milled,
- dry feed or digesta were extracted in 5 mL of 100 mM NaF, 20 mM Na₂EDTA (pH 10) for 30 minutes
- 422 shaking, followed by 30 minutes in a chilled bath sonicator and a further 2 hours standing at 4°C. The
- 423 extract was centrifuged at 9000 x g for 15 minutes at 4°C and 1 mL was filtered through a 13-mm
- 424 0.45μm PTFE syringe filter (Kinesis, UK). Aliquots (20 μL) were analysed by HPLC with UV detection at
- 425 290 nm after post-column complexation of inositol phosphates with ferric ion.
- 426 Analysis of inositol phosphates in gut tissues

- Tissue (100 mg frozen weight) was homogenised with an Ultra-Turrax (IKA T-10 Ultra-Turrax® High-
- 428 Speed Homogeniser) with 8 mm stainless steel probe (S 10 N 8 G ST) in 600 μL 1M HClO₄ in a Pyrex
- 429 glass tube on ice. After transfer to 1.5 mL tubes, the samples were held on ice for 20 minutes with
- 430 vortexing at 10-minute intervals and centrifuged at 13,000 x g for 10 minutes at 4°C. Following
- removal of an aliquot (20 μL) which was diluted to 1000 μL with 18.2 Megohm.cm water for analysis
- of inositol, the cleared lysates were applied to titanium dioxide (TiO_2) beads (Titansphere® TiO_2 5 μ M,
- 433 Hichrom) (73).
- 434 Analysis of inositol phosphates recovered from TiO₂
- Perchloric acid extracts, in their entirety, minus the aliquot taken for inositol analysis, were applied
- 436 to 5 mg of titanium dioxide (TiO₂) beads (Titansphere® TiO₂ 5 μM, Hichrom) and incubated for 30
- 437 minutes with mixing on a rotator. Thereafter, samples were centrifuged at 3500 x q for 5 minutes
- and the HClO₄ supernatant was discarded. Inositol phosphates were eluted from beads resuspended
- in 200 μL 3% ammonium hydroxide solution (pH 10), with vortexing and incubation for 5 minutes at
- 440 4°C. After centrifugation, 3500 x g for 1 minute, the supernatant was transferred to a clean 1.5 mL
- tube and the beads were further extracted with a second 200 μL aliquot of ammonium hydroxide
- 442 (73). The eluates were pooled, freeze-dried until dry and resuspended in 100 μL of 18.2MOhm.cm
- 443 water for further analysis by HPLC.
- 444 Funding
- 445 This study was funded by award of a BBSRC Norwich Research Park Doctoral Training Studentship
- 446 (Ref. BB/M011216/1) to C.S. with contribution from AB Vista and a NERC grant NE/W000350/1 to
- 447 C.A.B. and H.W. Feeding trials described in this study were designed by AB Vista and commissioned

- at Nottingham Trent University by AB Vista. BVLP is a Wellcome Trust Senior Investigator (grant
- 449 101010). AS is supported by the Medical Research Council grant MR/T028904/1.
- 450 Author Contributions
- This work was funded in part by the Wellcome Trust. For the purpose of Open Access, the authors
- 452 have applied a CC BY public copyright license to any author-accepted manuscript version arising
- 453 from this submission.
- 454 Acknowledgements
- 455 We thank Dirk Freese (Brandenburgische Technische Universität Cottbus-Senftenberg) for providing
- 456 soil samples, Joe Carroll (University of East Anglia) for extraction of the Bad Lauchstädt soil sample
- 457 and Graham Chilvers of the Science Analytical Facility (University of East Anglia) for operation of the
- 458 LC-ICP-MS. "Chicken (white leghorn)" by DataBase Center for Life Science (DBCLS), modified and
- 459 licensed under CC BY 4.0. "ArabidopsisTopView" by James-Lloyd, modified and licensed under CC0
- 460 <u>1.0.</u> "Scheme of the *Chlamydomonas reinhardtii* cell" by Nefronus, modified and licensed under <u>CCO</u>
- 461 1.0. "A diagram of a typical lawn grass plant" by Kelvinsong, modified and licensed under CC BY 3.0.
- 462 "Microtube Green" by Servier, modified and licensed under CC BY 4.0. "Liquid Chromatograph Mass
- Spectrometer" by DataBase Center for Life Science (DBCLS), modified and licensed under CC BY 4.0.
- We thank Holly Brearley for original artwork and Thomas Brearley for assistance with graphing.
- 465 Conflict of Interests Statement
- 466 AB Vista had no role in conducting the research, generating the data, interpreting the results of the
- study or writing the manuscript.
- 468 Data availability

470 <u>brearley/datasets/</u>

471 Figure Legends

Figure 1. Separation of PP-InsPs and InsPs by LC-ICP-MS. A. Cartoon of an LC-ICP-MS procedure applicable to diverse taxa and sample matrices. B. Simplified metabolic relationships of InsPs, PtdInsPs and PP-InsPs showing lipid-derived and 'soluble' contributions to PP-InsP synthesis. Arrows indicate that pools of metabolites at individual levels of phosphorylation are in exchange with each other. For some pools, the interconverting enzymes are reversible whereas for others different enzymes may operate. C. The complexity of InsP5 and PP-InsP5 speciation. For each, there are six possible stereoisomers of which four exist as two pairs of enantiomers (reflected here in a mirror plane). For both, the other two isomers (like InsP6) are meso-compounds: they possess an internal plane of symmetry between carbon 2 and carbon 5. D Analysis of an acid hydrolysate of myo-InsP6 (orange), and a 50-fold dilution thereof 'spiked' with 5-PP-Ins(1,3,4,6)P4, (5-PP-InsP4), 5-PP-InsP5, 1-PP-InsP5 and 1,5-[PP]2-InsP4 (red line). Samples were run on a CarboPac PA200 HPLC column eluted with a shallow linear gradient of HCl. Equivalent separations of the inositol pyrophosphate species from InsP4, InsP5 and InsP6 species shown here have been observed on more than 30 occasions on CarboPac PA200 column coupled to ICP-MS.

Figure 2. Separation of PP-InsPs and InsPs in Dictyostelium by LC-ICP-MS. A. A perchloric acid extract of *Dictyostelium discoideum* amoebae (blue trace) and an acid-hydrolysate of InsP₆ (orange trace). **B.** An expansion of the InsP₄ and InsP₅ region of the chromatogram shown in A. **C.** An expansion of the InsP₆ and PP-InsP region of the chromatogram shown in A (Dictyostelium extract, blue trace), with the same sample (at different concentration) spiked with 1-PP-InsP₅, 5-PP-InsP₅ and 1,5-[PP]₂-InsP₄ (green trace), and separately a set of the standards of InsP₆, 1-PP-InsP₅, 5-PP-InsP₅, 1,5-[PP]₂-InsP₄ (red trace). Compounds were resolved on a CarboPac PA200 column eluted with a positive exponential gradient of HCl. The PP-InsP peaks for which standards were not available, 4/6-PP-InsP₅ and 4/6,5-[PP]₂-InsP₄, are identified according to the known order of elution of PP-InsP₅s and 1/3-PP-InsP₅ eluted on CarboPac PA200 ^{22,23} and by reference to the characterization of Dictyostelium by CE-MS (Figure 4 of ¹⁶) which identifies 4/6,5-[PP]₂-InsP₄ as the principle PP-InsP species therein. Chromatography with resolution similar to this was observed on more than five different injections of different Dictyostelium samples.

Downloaded from http://portlandpress.com/biochem/jarticle-pdf/doi/10.1042/BCJ20253151/978745/bcj-2025-3151.pdf by University College London user on 14 October 2025

Figure 3. Resolution of inositol hexakisphosphates in soil. A. InsPs from a Chernozem soil analysed on a short, steep linear gradient (orange line). Individual standards of *neo*-InsP₆ (blue), D-*chiro*-InsP₆ (red), *myo*-InsP₆ (cyan) and *scyllo*-InsP₆ (green) are shown with their chemical structures. Resolution of soil samples equivalent to this has been observed on more than 100 occasions by LC-ICP-MS. **B.** A three-decade dilution of an InsP₆ hydrolysate. The aliquots injected are 10-, 100- and 1000-fold dilutions of the hydrolysate analysed in Figure 2C (analysed as 20 μL injection). The peak areas (counts.min) of the InsP₆ peak are 8,249,418, 813,719 and 86,360, respectively. **C.** Injections (10 μL) of InsP₆ dodecasodium salt. The peak areas (counts.min) of the InsP₆ peak are 6,301,172 at 50 μM and 1,055,441 at 10 μM. **D.** A calibration curve for phosphorus (Detector Response = peak area). Different amounts of phosphorus (single samples) were injected, as NaH₂PO₄, and the Pi peak integrated. For B, C, and D, single samples were analysed. Reproducibility for biological samples is further described in Figure S5.

Figure 4. LC-ICP-MS analysis of InsP₆ digestion in the avian gastrointestinal tract. LC-ICP-MS of lumenal ileal content of birds fed a diet containing low (500 FTU/kg) (blue) or high (6000 FTU/kg) (red) phytase. A hydrolysate of InsP₆ is shown (orange). The extract was resolved on a CarboPac PA200 column eluted with methanesulfonic acid. These individual chromatograms are representative, in terms of retention time and signal to noise ratio, of seven different tissue samples analysed in the middle of a set of more than 50 consecutive injections.

Figure 5. LC-ICP-MS analysis of tissue InsPs. A. Cartoon of chicken digestive tract and tissues analysed: kidney (yellow), duodenum (cyan), jejunum (green) and ileum (purple). B. InsPs extracted from blood are shown (red) and standards (InsP₆ hydrolysate) are shown (orange). **C**. InsPs of tissues: duodenum (cyan), ileum (purple). D. InsPs of tissues: jejunum (green) and kidney (yellow). E. Established pathway of InsP₆ synthesis in avian erythrocytes after Stephens and Downes ³⁰. The identities of InsP1 and InsP2 species are not well characterized. For B, whole blood from a 35d-old broiler was extracted in perchloric acid and diluted with NaF-EDTA. For C and D, InsPs extracted from tissues with perchoric acid were concentrated on TiO₂ prior to LC-ICP-MS. For B and C/D, chromatography was performed on separate HPLC machines on separate CarboPac PA200 columns eluted with gradients of HCI. The chromatograms shown were obtained from tissues of birds fed a control diet, lacking phytase. Separations of inositol phosphates on the CarboPac PA200 column matching the resolution shown (B,C,D) have been observed on more than 100 occasions for blood, on more than 50 occasions each for duodenum, ileum, jejunum and kidney tissues by LC-UV. For the ICP-MS analysis shown, the coefficient of variation of retention time of e.g., the InsP₅ [2-OH] peak is less than 1% across more than 10 runs across different tissues. A set of six blood samples is shown in Figure S2.

Figure 6. Modulation of gut tissue InsPs by diet. InsPs extracted from duodenum, jejunum and ileum tissues of broiler chickens fed different diets were analysed by HPLC. The diets comprise a control diet and the same supplemented with 2g/kg *myo*-inositol or 500 or 6000 FTU/kg phytase. 2g/kg inositol represents the amount of inositol that could be released in total from the InsP₆ content of the control feed. Individual faded points represent individual InsP measures. Large symbols and error bars represent estimated mean and 95% confidence intervals calculated by a general linear mixed model. The contrasts generated by the mixed model are shown in Table S1.

Downloaded from http://portlandpress.com/biochem/jarticle-pdf/doi/10.1042/BCJ20253151/978745/bcj-2025-3151.pdf by University College London user on 14 October 2025

Figure 7. Inositol phosphate profiles of wild-type (Col0) and PSR mutants. Plants grown for 12 weeks on soil were weighed, frozen in liquid N_2 , ground and extracted with perchloric acid. The extract was applied to TiO_2 , recovered with NH_4OH , lyophilized and recovered in 300 μ L of water. A 42.5 μ L aliquot was applied to LC-ICP-MS. The masses of the plants from which extracts were prepared are shown for each genotype: Col0 (blue), *pho2-1*, (red), *mrp5-2* (green), *ipk1* (purple).

Abbreviations

IPK1, IP5K, inositol pentakisphosphate 2-kinase; ITPK, inositol tris/tetrakisphosphate kinase; D-chiro-InsP₆, 1-D- chiro-inositol 1,2,3,4,5,6-hexakisphosphate; EDTA, ethylenediamine tetra-acetic acid; HEPES, 4-(2-hydroxyethyl)-1-piperazineethane sulfonic acid; His, histidine; HPLC, high-pressure liquid chromatography; IP6K, inositol hexakisphosphate kinase; Ins(1,2,3,4)P₄, 1D-myo-inositol 1,2,3,4-tetrakisphosphate; Ins(1,2,3,5)P₄, myo-inositol 1,2,3,5-tetrakisphosphate; Ins(1,3,4,5)P₄, 1D-myo-inositol 1,4,5,6-tetrakisphosphate; Ins(2,3,4,5)P₄, 1D-myo-inositol 2,3,4,5-tetrakisphosphate; Ins(2,3,4,6)P₄, 1D-myo-inositol 2,3,4,6-tetrakisphosphate; Ins(2,4,5,6)P₄, myo-inositol 2,4,5,6-tetrakisphosphate; Ins(3,4,5,6)P₄, 1D-myo-inositol 2,4,5,6-t

inositol 3,4,5,6-tetrakisphosphate; InsP₅ [1-OH], Ins(2,3,4,5,6)P₅, 1D-myo-inositol 2,3,4,5,6pentakisphosphate; InsP₅ [2-OH], Ins(1,3,4,5,6)P₅, myo-inositol 1,3,4,5,6-pentakisphosphate; InsP₅ [3-OH], Ins(1,2,4,5,6)P₅, 1D-myo-inositol 1,2,4,5,6-pentakisphosphate; InsP₅ [4-OH], Ins(1,2,3,5,6)P₅, 1D-myo-inositol 1,2,3,5,6-pentakisphosphate; $InsP_5$ [5-OH], $Ins(1,2,3,4,6)P_5$, myo-inositol 1,2,3,4,6pentakisphosphate; InsP₅ [6-OH], Ins(1,2,3,4,5)P₅, 1D-myo-inositol 1,2,3,4,5-pentakisphosphate; InsP₆, Ins(1,2,3,4,5,6)P₆, myo-inositol 1,2,3,4,5,6-hexakisphosphate; 3-PP-Ins(1,2,4,5)P₄, 1D-3-diphosphomyo-inositol 1,2,4,5-tetrakisphosphate; 5-PP-Ins(1,2,3,4)P₄, 1D-5-diphospho-myo-inositol 1,2,3,4tetrakisphosphate; 1-InsP₇, 1-PP-InsP₅, 1D-1-diphospho-myo-inositol 2,3,4,5,6-pentakisphosphate; 2-InsP₇, 2-PP-InsP₅, 2-diphospho-myo-inositol 1,3,4,5,6-pentakisphosphate; 3-InsP₇, 3-PP-InsP₅, 1D-3diphospho-myo-inositol 1,2,4,5,6-pentakisphosphate; 4-InsP₇, 4-PP-InsP₅, 1D-4-diphospho-myoinositol 1,3,5,6-pentakisphosphate; 5-InsP₇, 5-PP-InsP₅, 5-diphospho-myo-inositol 1,2,3,4,6pentakisphosphate; 6-InsP₇, 6-PP-InsP₅, 1D-6-diphospho-myo-inositol 1,2,3,4,5-pentakisphosphate; InsP₈, bis-diphospho-myo-inositol-tetrakisphosphate; 1,5-InsP₈, 1D-1,5-bis-diphospho-myo-inositol 2,3,4,6-tetrakisphosphate; 3,5-InsP₈, 1D-3,5-bis-diphospho-myo-inositol 1,2,4,6-tetrakisphosphate; 4,5-InsP₈, 1D-4,5-bis-diphospho-myo-inositol 1,2,3,6-tetrakisphosphate; 6,5-InsP₈, 1D-6,5-bisdiphospho-myo-inositol 1,2,3,4-tetrakisphosphate; neo-InsP₆, neo-inositol 1,2,3,4,5,6hexakisphosphate; rac-InsP₈, 1:1 mixture of 1,5-InsP₈ and 3,5-InsP₈; scyllo-InsP₆, scyllo-inositol 1,2,3,4,5,6-hexakisphosphate. VIH, Arabidopsis thaliana diphosphoinositol pentakisphosphate.

References

- Mukherjee, S., Haubner, J., Chakraborty, A. Targeting the inositol pyrophosphate biosynthetic enzymes in metabolic diseases. *Molecules* 25, (2020). 10.3390/molecules25061403
- Lee, B., Park, S.J., Hong, S., Kim, K., Kim, S. Inositol polyphosphate multikinase signaling: multifaceted functions in health and disease. *Mol Cells* 44, 187-194 (2021). 10.14348/molcells.2021.0045
- 3. Tu-Sekine, B., Kim, S.F. The inositol phosphate system a coordinator of metabolic adaptability. *Int J Mol Sci* **23**, (2022). 10.3390/ijms23126747
- 4. Kim, S., Bhandari, R., Brearley, C.A., Saiardi, A. The inositol phosphate signalling network in physiology and disease. Trends Biochem Sci *49*, 969-985 (2024). 10.1016/j.tibs.2024.08.005
- Gibson, R.S., Bailey, K.B., Gibbs, M., Ferguson, E.L. A review of phytate, iron, zinc, and calcium concentrations in plant-based complementary foods used in low-income countries and implications for bioavailability. *Food Nutr Bull* 31, S134-146 (2010). 10.1177/15648265100312S206
- Michaelsen, K.F. Complementary feeding of young children in developing countries: a review of current scientific knowledge: edited by Kenneth Brown, Kathryn Dewey, and Lindsay Allen, 1998, 178 pages, softcover. World Health Organization, Geneva. *The American Journal of Clinical Nutrition* 71, 605-606 (2000).10.193/acjn/71.2.605a
- 7. Guha, P., Tyagi, R., Chowdhury, S., Reilly, L., Fu, C., Xu, R, et al. IPMK mediates activation of ULK signaling and transcriptional regulation of autophagy linked to liver inflammation and regeneration. *Cell Rep* **26**, 2692-2703 e2697 (2019). 10.1016/j.celrep.2019.02.013
- 8. Kim, E., Beon, J., Lee, S., Park, S.J., Ahn, H., Kim, M.G, et al. Inositol polyphosphate multikinase promotes Toll-like receptor-induced inflammation by stabilizing TRAF6. *Sci Adv* **3**, e1602296 (2017). 10.1126/sciadv.1602296

9.

10.

1143 (2003). 10.1038/ni980

10.3382/ps/pex390

21.

multikinase. Gastroenterology 149, 67-78 (2015). 10.1053/j.gastro.2015.04.008 11. Croze, M.L., Soulage, C.O. Potential role and therapeutic interests of myo-inositol in metabolic diseases. Biochimie 95, 1811-1827 (2013). 10.1016/j.biochi.2013.05.011 Downloaded from http://portlandpress.com/biochemi/article-pdf/doi/10.1042/BCJ20253151/978745/bcj-2025-3151.pdf by University College London user on 14 October 2025 12. Chang, H.H., Chao, H.N., Walker, C.S., Choong, S.Y., Phillips, A., Loomes, K.M. Renal depletion of myo-inositol is associated with its increased degradation in animal models of metabolic disease. Am J Physiol Renal Physiol 309, F755-763 (2015). 10.1152/ajprenal.00164.2015 13. Moritoh, Y., Abe, S.I., Akiyama, H., Kobayashi, A., Koyama, R., Hara, R, et al. The enzymatic activity of inositol hexakisphosphate kinase controls circulating phosphate in mammals. Nat Commun 12, 4847 (2021). 10.1038/s41467-021-24934-8 14. Park, S.E., Lee, D., Jeong, J.W., Lee, S.H., Park, S.J., Ryu, J, et al. Gut epithelial inositol polyphosphate multikinase alleviates experimental Colitis via governing Tuft cell homeostasis. Cell Mol Gastroenterol Hepatol 14, 1235-1256 (2022). 10.1016/j.jcmgh.2022.08.004 15. Bevilacqua, A., Dragotto, J., Lucarelli, M., Di Emidio, G. Monastra, G., Tatone, C. High doses of D-chiro-inositol alone induce a PCO-Like syndrome and other alterations in mouse ovaries. Int J Mol Sci 22, (2021). 10.3390/ijms22115691 Mayr, G.W. A novel metal-dye detection system permits picomolar-range h.p.l.c. analysis of 16. inositol polyphosphates from non-radioactively labelled cell or tissue specimens. Biochem J 254, 585-591 (1988). 10.1042/bj2540585 17. Qiu, D., Wilson, M.S., Eisenbeis, V.B., Harmel, R.K., Riemer, E., Haas, T.M, et al. Analysis of inositol phosphate metabolism by capillary electrophoresis electrospray ionization mass spectrometry. Nat Commun 11, 6035 (2020). 10.1038/s41467-020-19928-x 18. Clases, D., Gonzalez de Vega, R. Facets of ICP-MS and their potential in the medical sciences-Part 1: fundamentals, stand-alone and hyphenated techniques. Anal Bioanal Chem 414, 7337-7361 (2022). 10.1007/s00216-022-04259-1 19. Carroll, J.J., Sprigg, C., Chilvers, G., Delso, I., Barker, M., Cox, F, et al. LC-ICP-MS analysis of inositol phosphate isomers in soil offers improved sensitivity and fine-scale mapping of inositol phosphate distribution. Methods in Ecology and Evolution 15, 530-543 (2024). 10.1111/2041-210X.14292 20. Sommerfeld, V., Kunzel, S., Schollenberger, M., Kuhn, I., Rodehutscord, M. Influence of phytase or myo-inositol supplements on performance and phytate degradation products in the crop, ileum, and blood of broiler chickens. Poult Sci 97, 920-929 (2018).

Pouillon, V., Hascakova-Bartova, R., Pajak, B., Adam, W., Bex, F., Dewaste, V, et al. Inositol 1,3,4,5-tetrakisphosphate is essential for T lymphocyte development. *Nat Immunol* **4**, 1136-

Sei, Y., Zhao, X., Forbes, J., Szymczak, S., Li, Q., Trivedi, A, et al. A hereditary form of small

intestinal carcinoid associated with a germline mutation in inositol polyphosphate

22. Furness, J.B., Rivera, L.R., Cho, H.J., Bravo, D.M., Callaghan, B. The gut as a sensory organ. Nat Rev Gastroenterol Hepatol 10, 729-740 (2013). 10.1038/nrgastro.2013.180

Sommerfeld, V., Schollenberger, M., Kuhn, I., Rodehutscord, M. Interactive effects of phosphorus, calcium, and phytase supplements on products of phytate degradation in the digestive tract of broiler chickens. *Poult Sci* **97**, 1177-1188 (2018). 10.3382/ps/pex404

- 23. Whitfield, H., White, G., Sprigg, C., Riley, A.M, Potter, B.V.L., Hemmings, A.M, et al. An ATPresponsive metabolic cassette comprised of inositol tris/tetrakisphosphate kinase 1 (ITPK1) and inositol pentakisphosphate 2-kinase (IPK1) buffers diphosphoinositol phosphate levels. Biochemical Journal 477, 2621-2638 (2020). 10.1042/BCJ20200423
- 24. Whitfield, H.L., Rodriguez, R.F., Shipton, M.L., Li, A.W.H., Riley, A.M., Potter, B.V.L, et al. Crystal structure and enzymology of Solanum tuberosum inositol tris/tetrakisphosphate kinase 1 (StITPK1). Biochemistry 63, 42-52 (2024). 10.1021/acs.biochem.3c00404
- 25. Greiner, R., Konietzny, U., Jany, K.D. Purification and characterization of two phytases from Escherichia coli. Arch Biochem Biophys 303, 107-113 (1993). 10.1006/abbi.1993.1261
- 26. Madsen, C.K., Dionisio, G., Holme, I.B., Holm, P.B., Brinch-Pedersen, H. High mature grain phytase activity in the Triticeae has evolved by duplication followed by neofunctionalization of the purple acid phosphatase phytase (PAPhy) gene. J Exp Bot 64, 3111-3123 (2013). 10.1093/jxb/ert116
- 27. Faba-Rodriguez, R., Gu, Y., Salmon, M., Dionisio, G., Brinch-Pedersen, H., Brearley, C.A. et al. Structure of a cereal purple acid phytase provides new insights to phytate degradation in plants. Plant Commun 3, 100305 (2022). 10.1016/j.xplc.2022.100305
- 28. Sprigg, C., Whitfield, H., Burton, E., Scholey, D., Bedford, M. R., Brearley, C.A. Phytase dosedependent response of kidney inositol phosphate levels in poultry. PLoS One 17, e0275742 (2022). 10.1371/journal.pone.0275742
- 29. Arthur, C., Rose, S., Mansbridge, S.C. Brearley, C., Kühn, I., Pirgozliev, V. The correlation between myo-inositol (Ins) concentration in the jejunum digesta of broiler chickens and the Ins concentrations of key tissues associated with the uptake and regulation of Ins. British Poultry Abstracts 17, 1-29 (2021). 10.1080/17466202.2021.1983311

- 30 Stephens, L.R., Downes, C.P. Product-precursor relationships amongst inositol polyphosphates. Incorporation of [32P]Pi into myo-inositol 1,3,4,6-tetrakisphosphate, myoinositol 1,3,4,5-tetrakisphosphate, myo-inositol 3,4,5,6-tetrakisphosphate and myo-inositol 1,3,4,5,6-pentakisphosphate in intact avian erythrocytes. Biochem J 265, 435-452 (1990). 10.1042/bj2650435
- 31. Mayr, G.W., Dietrich, W. The only inositol tetrakisphosphate detectable in avian erythrocytes is the isomer lacking phosphate at position 3: a NMR study. FEBS Lett 213, 278-282 (1987). 10.1016/0014-5793(87)81505-3
- 32. Irvine, R.F., Schell, M.J. Back in the water: the return of the inositol phosphates. Nat Rev Mol Cell Biol 2, 327-338 (2001). 10.1038/35073015
- 33. Konietzny, U., Greiner, R. Molecular and catalytic properties of phytate-degrading enzymes (phytases). International Journal of Food Science & Technology 37, 791-812 (2002). 10.1046/j.1365-2621.2002.00167.x
- 34. Stentz, R., Osborne, S., Horn, N., Li, A.W., Hautefort, I., Bongaerts, R, et al. A bacterial homolog of a eukaryotic inositol phosphate signaling enzyme mediates cross-kingdom dialog in the mammalian gut. Cell Rep 6, 646-656 (2014). 10.1016/j.celrep.2014.01.021
- 35. Trung, M.N., Kieninger, S., Fandi, Z., Qiu, D., Liu, G., Mehendale, N.K, et al. Stable isotopomers of myo-inositol uncover a complex MINPP1-dependent inositol phosphate network. ACS Central Science 8, 1683-1694. 2022.2008.2029.505671 (2022). 10.1021/acscentsci.2c01032

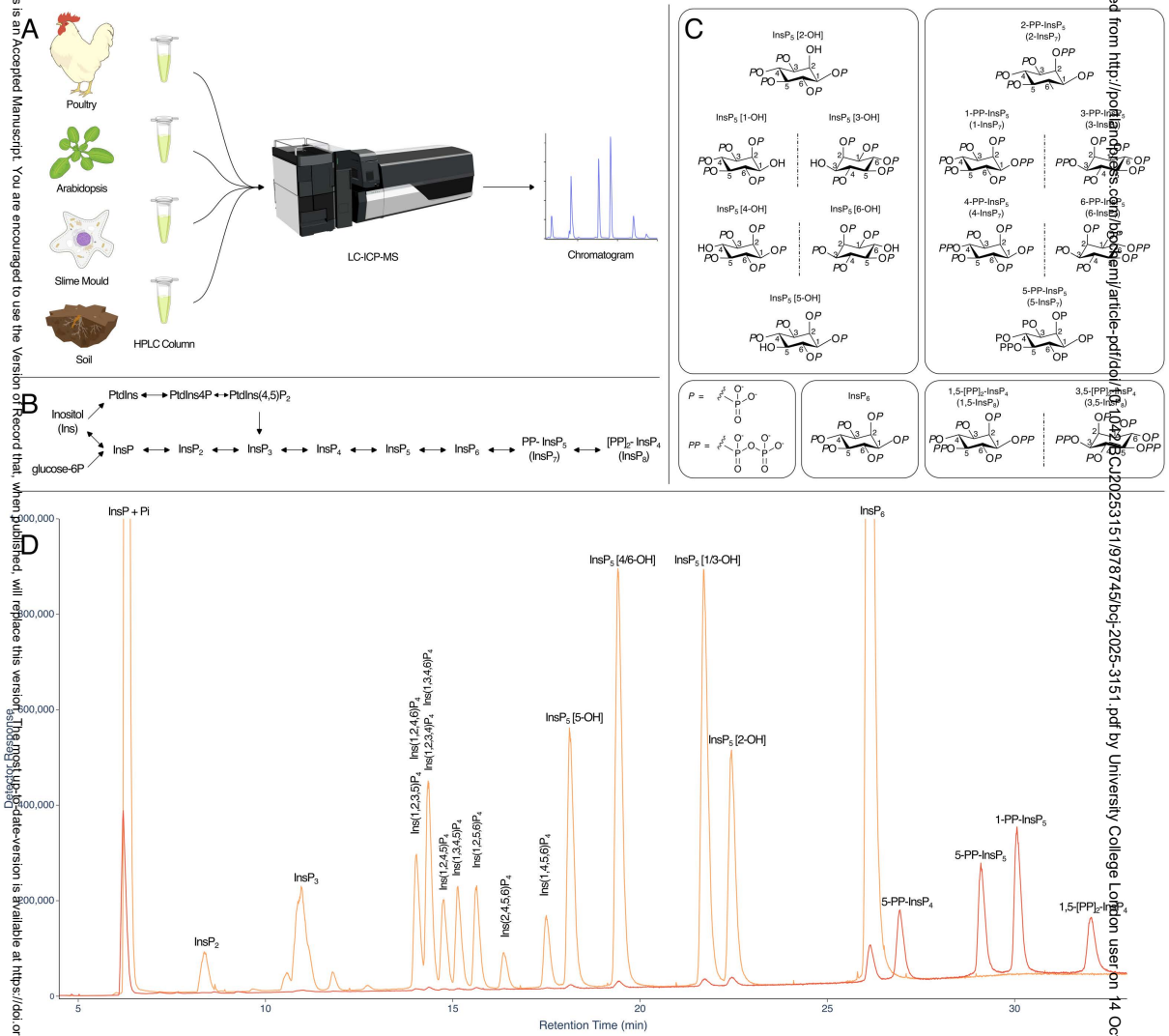
- 36. Turner, B.L., Paphazy, M.J., Haygarth, P.M., McKelvie, I.D. Inositol phosphates in the environment. Philos Trans R Soc Lond B Biol Sci 357, 449-469 (2002). 10.1098/rstb.2001.0837
- 37. Martin, J.B., Laussmann, T., Bakker-Grunwald, T., Vogel, G., Klein, G. neo-inositol polyphosphates in the amoeba Entamoeba histolytica. J Biol Chem 275, 10134-10140 (2000). 10.1074/jbc.275.14.10134.
- 38. De Vos, W.M., Trung, M.N., Davids, M., Liu, G., Rios-Morales, M., Jessen, H, et al. Phytate metabolism is mediated by microbial cross-feeding in the gut microbiota. Nature Microbiology 9, 1812-1827 (2024). 10.1038/s41564-024-01698-7
- 39. Qiu, D., Gu, C., Liu, G., Ritter, K., Eisenbeis, V.B., Bittner, T, et al. Capillary electrophoresis mass spectrometry identifies new isomers of inositol pyrophosphates in mammalian tissues. Chem Sci 14, 658-667 (2023). 10.1039/d2sc05147h
- 40 Ito, M., Fujii, N., Wittwer, C., Sasaki, A. Tanaka, M., Bittner, T, et al. Hydrophilic interaction liquid chromatography-tandem mass spectrometry for the quantitative analysis of mammalian-derived inositol poly/pyrophosphates. J Chromatogr A. 1573:87-97 (2018). 10.1016/j.chroma.2018.08.061
- 41 Ito, M., Fujii, N., Kohara, S., Hori, S., Tanaka, M., Wittwer, C, et al. Inositol pyrophosphate profiling reveals regulatory roles of IP6K2-dependent enhanced IP7 metabolism in the enteric nervous system. J Biol Chem. 299(3):102928 (2023). 10.1016/j.jbc.2023.102928
- 42. Cowieson, A.J., Ruckebusch, J.P., Sorbara, J.O.B., Wilson, J.W., Guggenbuhl, P., Roos, F.F. A systematic review on the effect of phytase on ileal amino acid digestibility in broilers. Animal Feed Science and Technnology 225, 182-194 (2017). 10.1016/j.anifeedsci.2017.01.008.

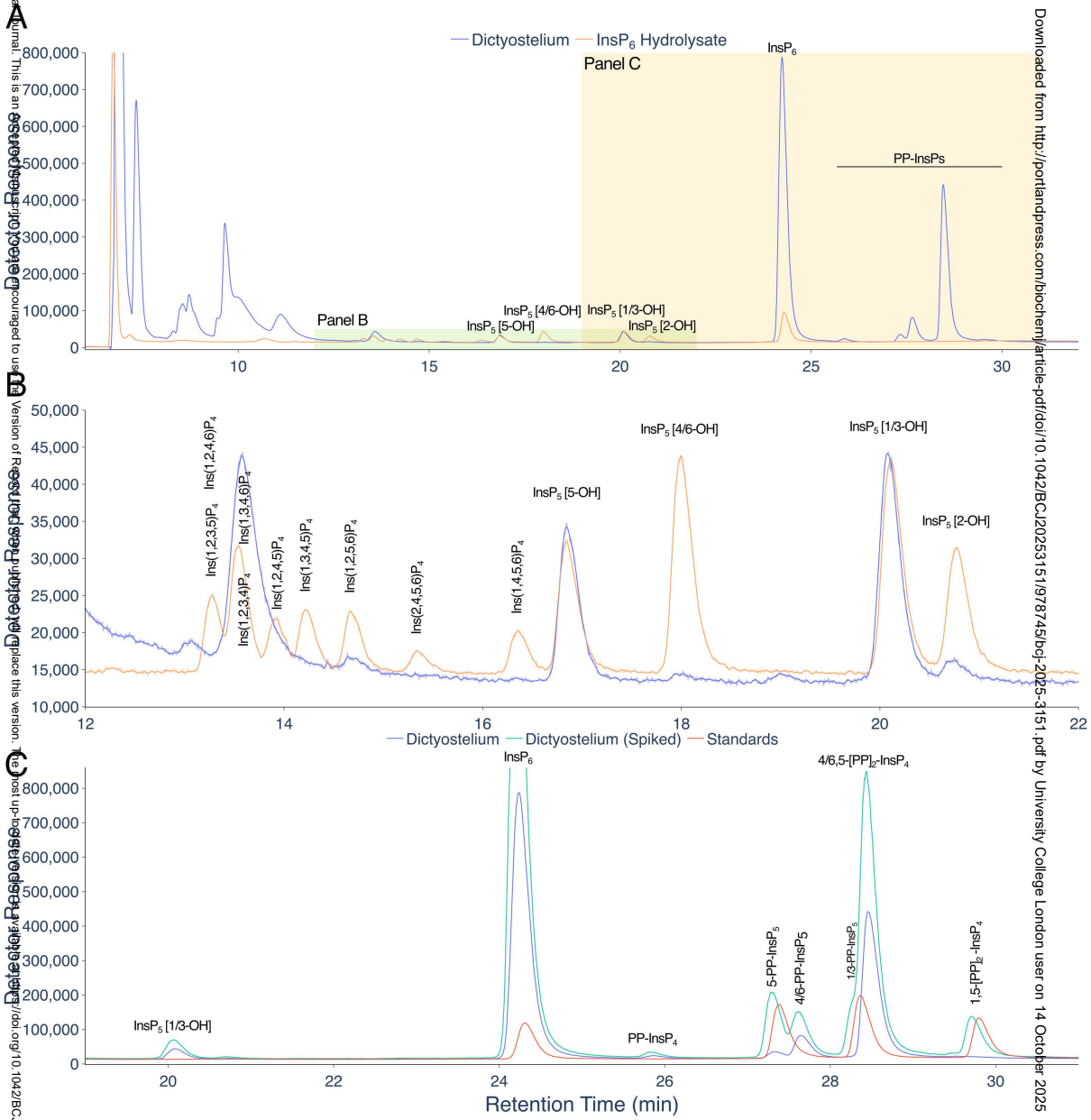
- 43. Sprigg, C., Leftwich, P.T., Burton, E., Scholey, D., Bedford, M.R., Brearley, C.A. Accentuating the positive and eliminating the negative: Efficacy of TiO₂ as digestibility index marker for poultry nutrition studies. PLoS One 18, e0284724 (2023). 10.1371/journal.pone.0284724
- 44. Phillippy, B.Q., Ullah, A.H., Ehrlich, K.C. Purification and some properties of inositol 1,3,4,5,6pentakisphosphate 2-kinase from immature soybean seeds. J Biol Chem 269, 28393-28399 (1994). 10.1016/S0021-9258(18)46940-2.
- 45. Kuo, H.F., Hsu, Y.Y., Lin, W.C., Chen, K.Y., Munnik, T., Brearley, C.A, et al. Arabidopsis inositol phosphate kinases, IPK1 and ITPK1, constitute a metabolic pathway in maintaining phosphate homeostasis. The Plant Journal 95, 613-630 (2018). 10.1111/tpj.13974
- 46. Kuo, H.F., Chang, T.Y., Chiang, S.F., Wang, W.D., Charng, Y.Y., Chiou, T.J. Arabidopsis inositol pentakisphosphate 2-kinase, AtIPK1, is required for growth and modulates phosphate homeostasis at the transcriptional level. Plant J 80, 503-515 (2014). 10.1111/tpj.12650
- 47. Stevenson-Paulik, J., Bastidas, R.J., Chiou, S.T., Frye, R.A., York, J.D. Generation of phytatefree seeds in Arabidopsis through disruption of inositol polyphosphate kinases. Proc Natl Acad Sci U S A 102, 12612-12617 (2005). 10.1073/pnas.0504172102
- 48. Wild, R., Gerasimaite, R., Jung, J.Y., Truffault, V., Pavlovic, I., Schmidt, A, et al. Control of eukaryotic phosphate homeostasis by inositol polyphosphate sensor domains. Science 352, 986-990 (2016). 10.1126/science.aad9858
- 49. Land, E.S., Cridland, C. A., Craige, B., Dye, A., Hildreth, S.B., Helm, R.F, et al. A role for inositol pyrophosphates in the metabolic adaptations to low phosphate in Arabidopsis. Metabolites **11**, (2021). 10.3390/metabo11090601

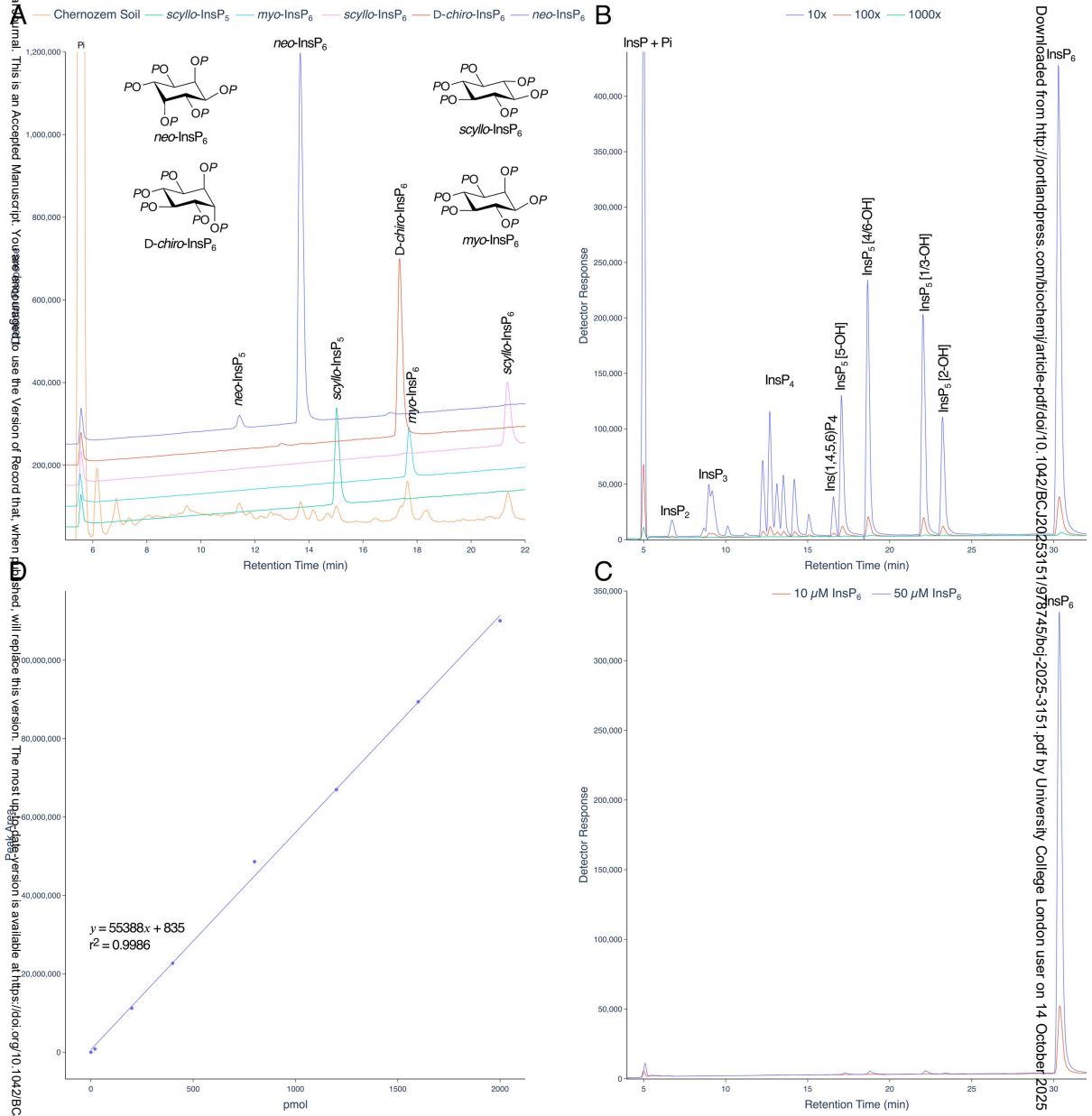
- 50 Yang, S.Y., Lin, W. Y., Hsiao, Y.M., Chiou, T.J. Milestones in understanding transport, sensing, and signaling of the plant nutrient phosphorus. Plant Cell. 36(5):1504-1523 (2024). 10.1093/plcell/koad326
- 51. Delhaize, E., Randall, P.J. Characterization of a phosphate-accumulator mutant of Arabidopsis thaliana. Plant Physiol 107, 207-213 (1995). 10.1104/pp.107.1.207
- 52. Aung, K., Lin, S.I., Wu, C.C., Huang, Y.T., Su, C.L., Chiou, T.J. pho2, a phosphate overaccumulator, is caused by a nonsense mutation in a microRNA399 target gene. Plant Physiol 141, 1000-1011 (2006). 10.1104/pp.106.078063
- 53. Gulabani, H., Goswami, K., Walia, Y., Roy, A., Noor, J.J., Ingole, K.D, et al. Arabidopsis inositol polyphosphate kinases IPK1 and ITPK1 modulate crosstalk between SA-dependent immunity and phosphate-starvation responses. Plant Cell Rep 41, 347-363 (2022). 10.1007/s00299-021-02812-3
- 54. Nagy, R., Grob, H., Weder, B., Green, P., Klein, M., Frelet-Barrand, A, et al. The Arabidopsis ATP-binding cassette protein AtMRP5/AtABCC5 is a high affinity inositol hexakisphosphate transporter involved in guard cell signaling and phytate storage. J Biol Chem 284, 33614-33622 (2009). 10.1074/jbc.M109.030247
- 55. Riemer, E., Qiu, D., Laha, D., Harmel, R.K., Gaugler, P., Gaugler, V, et al. ITPK1 is an InsP₆/ADP phosphotransferase that controls phosphate signaling in Arabidopsis. Mol Plant 14, 1864-1880 (2021). 10.1016/j.molp.2021.07.011
- 56. Buzas, EI. The roles of extracellular vesicles in the immune system. Nature Reviews Immunology 4, 236-250 (2023). 10.1038/s41577-022-00763-8
- Liu, G., Riemer, E., Schneider, R., Cabuzu, D., Bonny, O., Wagner, C.A, et al. The phytase 57. RipBL1 enables the assignment of a specific inositol phosphate isomer as a structural component of human kidney stones. RSC Chem Biol 4, 300-309 (2023). 10.1039/d2cb00235c

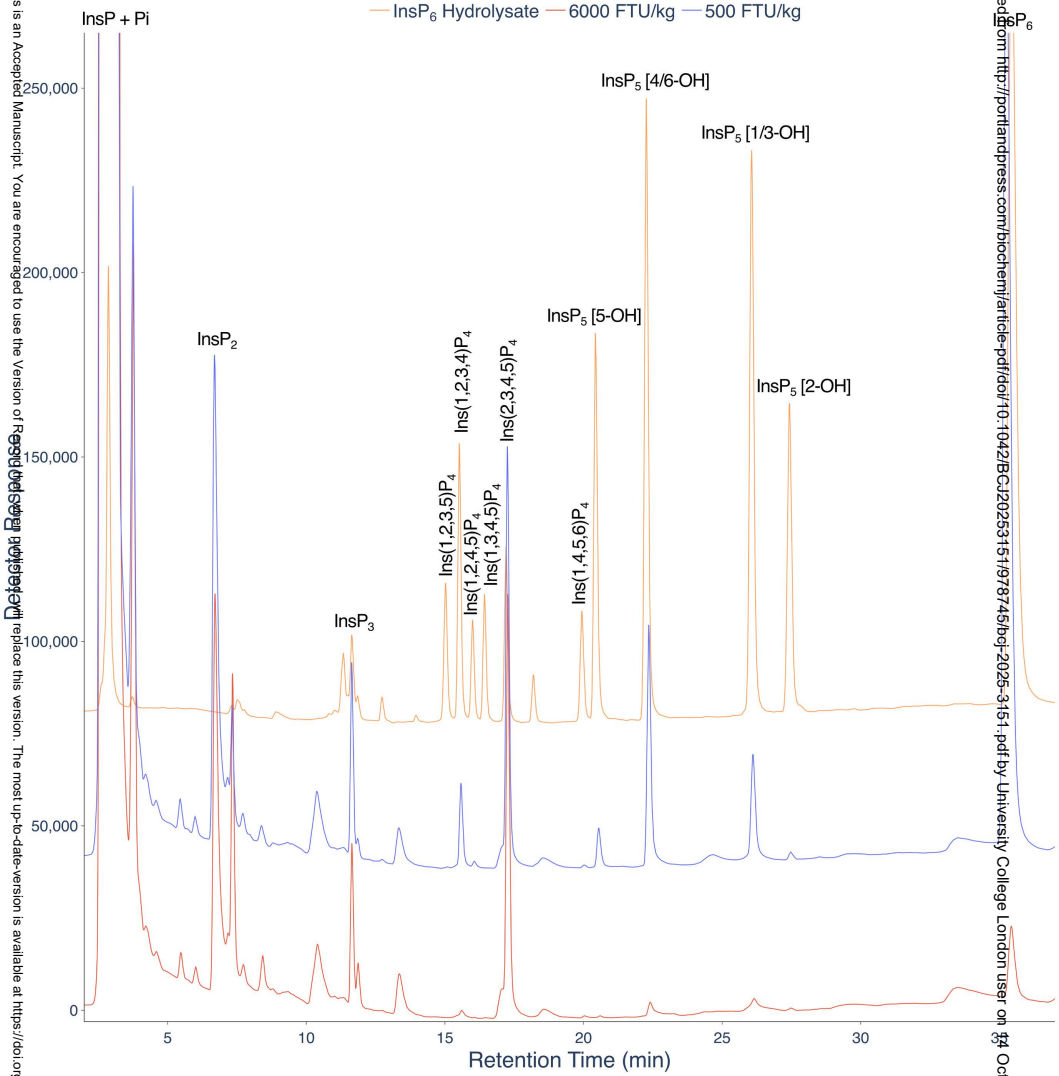
- 58. Casaravilla, C., Brearley, C., Soule, S., Fontana, C., Veiga, N., Bessio, M.I, et al. Characterization of myo-inositol hexakisphosphate deposits from larval Echinococcus granulosus. FEBS J 273, 3192-3203 (2006). 10.1111/j.1742-4658.2006.05328.x
- 59. Allaire, J.M., Crowley, S.M., Law, H.T., Chang, S.Y., Ko, H.J., Vallance, B.A. The intestinal epithelium: central coordinator of mucosal immunity. Trends Immunol 39, 677-696 (2018). 10.1016/j.it.2018.04.002
- 60. Gerbe, F., Jay, P. Intestinal Tuft cells: epithelial sentinels linking luminal cues to the immune system. Mucosal Immunol 9, 1353-1359 (2016). 10.1038/mi.2016.68
- Kim, W., Kim, E., Min, H., Kim, M.G., Eisenbeis, V.B., Dutta, A.K, et al. Inositol polyphosphates 61. promote T cell-independent humoral immunity via the regulation of Bruton's tyrosine kinase. Proc Natl Acad Sci U S A 116, 12952-12957 (2019). 10.1073/pnas.1821552116
- Reilly, L., Semenza, E.R., Koshkaryan, G., Mishra, S., Chatterjee, S., Abramson, E, et al. Loss of 62. PI3K activity of inositol polyphosphate multikinase impairs PDK1-mediated AKT activation, cell migration, and intestinal homeostasis. iScience 26, 106623 (2023). 10.1016/j.isci.2023.106623
- 63. Whitfield, H., Riley, A.M., Diogenous, S., Godage, H.Y., Potter, B.V.L., Brearley, C.A. Simple synthesis of (32)P-labelled inositol hexakisphosphates for study of phosphate transformations. Plant and Soil 427, 149-161 (2018). 10.1007/s11104-017-3315-9

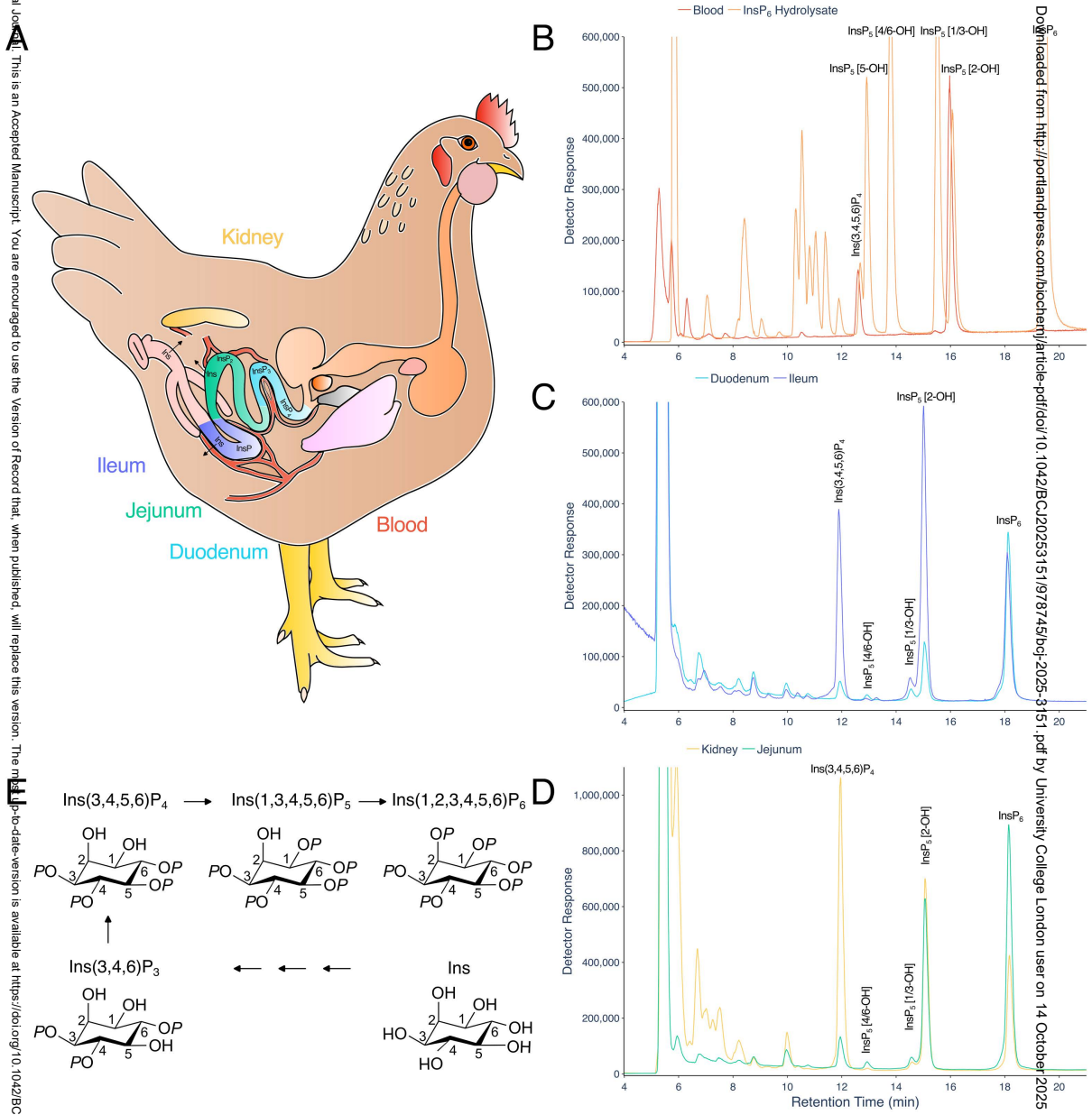
- 64. Riley, A.M., Wang, H., Weaver, J.D., Shears, S.B., Potter, B.V.L. First synthetic analogues of diphosphoinositol polyphosphates: interaction with PP-InsP₅ kinase. *Chem Commun (Camb)* **48**, 11292-11294 (2012). 10.1039/c2cc36044f
- 65. Brown, N.W., Marmelstein, A.M., Fiedler, D. Chemical tools for interrogating inositol pyrophosphate structure and function. *Chem Soc Rev* **45**, 6311-6326 (2016). 10.1039/c6cs00193a
- 66. Phillippy, B.Q., Bland, J.M. (1988) Gradient ion chromatography of inositol phosphates. *Anal Biochem* **175**, 162-166. 10.1016/0003-2697(88)90374-0.
- 67. Madsen, C.K., Brearley, C.A., Brinch-Pedersen, H. (2019) Lab-scale preparation and QC of phytase assay substrate from rice bran. *Anal Biochem* **578**, 7-12. 10.1016/j.ab.2019.04.021
- 68. R Core Team: A language and Environment for Statistical Computing. (2021).
- 69. Kuznetsova, A., Brockhoff, P.B., Christensen, R.H.B. ImerTest package: tests in linear mixed effects models. *Journal of Statistical Software* **82**, 26 (2017). 10.18637/jss.v082.i13
- 70. Lenth, R. emmeans: Estimated marginal means, aka least-squares means.) (2020).
- 71. Hartig F. DHARMa: Residual diagnostics for hierarchical (multi-level/mixed) regression models. (2020).
- 72. Walk, C.L., Bedford, M.R., Olukosi, O.A. Effect of phytase on growth performance, phytate degradation and gene expression of *myo*-inositol transporters in the small intestine, liver and kidney of 21day old broilers. *Poult Sci.* 2018; **97**(4):1155–62. 10.3382/ps/pex392
- 73. Wilson, M.S., Bulley, S.J., Pisani, F., Irvine, R.F., Saiardi, A. (2015) A novel method for the purification of inositol phosphates from biological samples reveals that no phytate is present in human plasma or urine. *Open Biol* **5**, 150014. 10.1098/rsob.150014

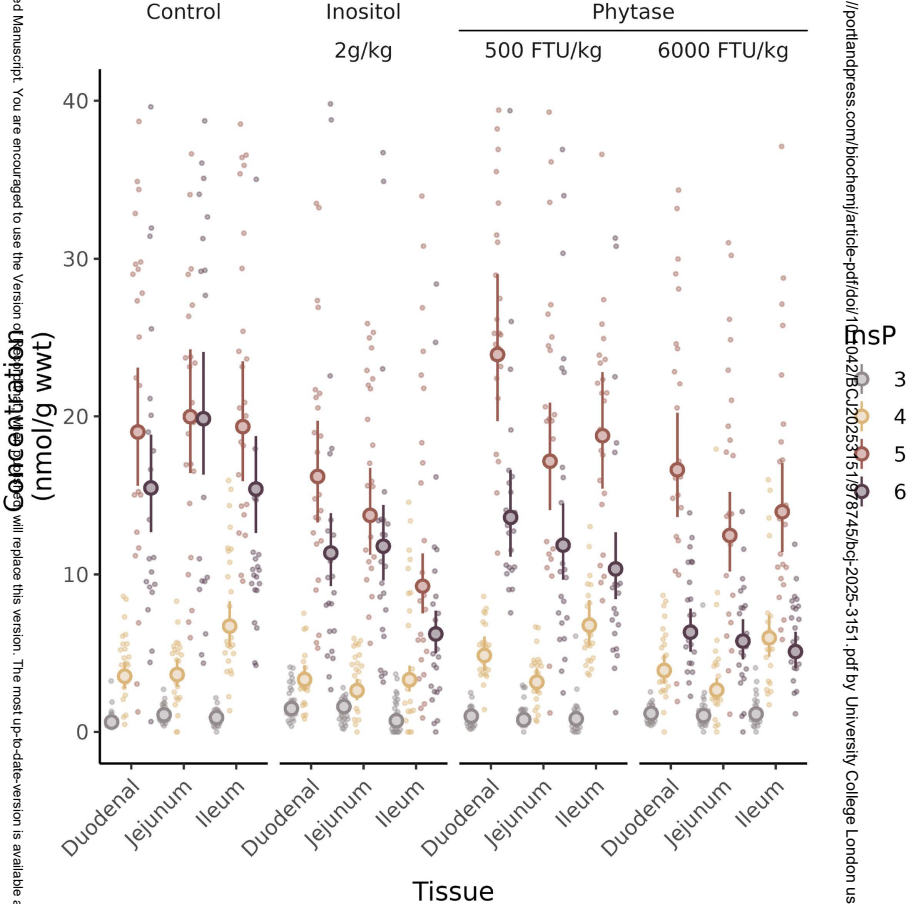


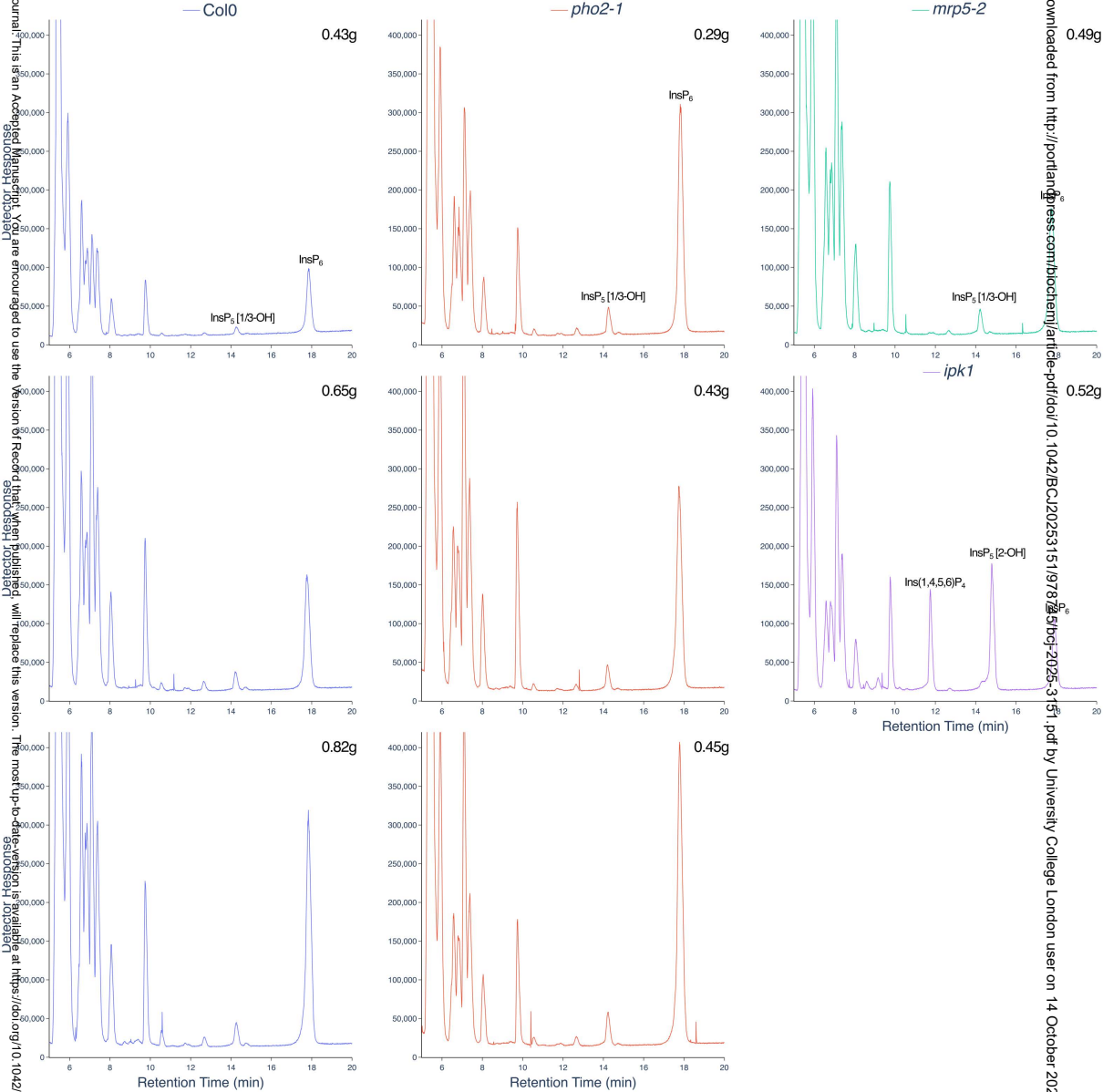












- 3 Phosphorus-specific, liquid chromatography inductively coupled plasma mass-spectrometry
- 4 for analysis of inositol phosphate and inositol pyrophosphate metabolism
- ¹Colleen Sprigg, ¹Hayley Whitfield, ¹Philip T. Leftwich, ²Hui-Fen Kuo, ²Tzyy-Jen Chiou, ³Adolfo Saiardi,
- ⁴Megan L. Shipton, ⁴Andrew M. Riley, ⁴Barry V.L. Potter, ⁵Dawn Scholey, ⁵Emily Burton, ⁶Mike R.
- 7 Bedford, ¹Charles A. Brearley
- ¹School of Biological Sciences, University of East Anglia, Norwich Research Park, Norwich NR4 7TJ, UK;
- ⁹ Agricultural Biotechnology Research Center, Academia Sinica, Taipei 115, Taiwan;
- ³Laboratory for Molecular Cell Biology, University College London, London WC1E 6BT, UK;
- ⁴Medicinal Chemistry & Drug Discovery, Department of Pharmacology, University of Oxford,
- 12 Mansfield Road, Oxford OX1 3QT, UK;
- 13 ⁵School of Animal, Rural and Environmental Sciences, Nottingham Trent University, Southwell,

Downloaded from http://portlandpress.com/biochem/jarticle-pdf/doi/10.1042/BCJ20253151/978745/bcj-2025-3151.pdf by University College London user on 14 October 2025

- 14 Nottingham NG25 0QF, UK;
- 15 ⁶AB Vista, Marlborough SN8 4AN, UK

16

- 17 Michael R. Bedford orcid.org/0000-0002-5308-4290
- 18 Charles A. Brearley; orcid.org/0000-0001-6179-9109
- 19 Emily Burton; orcid.org/0000-0003-2784-6922
- 20 Tzyy-Jen Chiou; orcid.org/0000-0001-5953-4144
- 21 Philip T. Leftwich; orcid.org/0000-0001-9500-6592
- 22 Barry V.L. Potter; orcid.org/0000-0003-3255-9135
- 23 Andrew M. Riley; orcid.org/0000-0001-9003-3540
- 24 Adolfo Saiardi; orcid.org/0000-0002-4351-0081
- 25 Megan L. Shipton; orcid.org/0000-0002-9982-0927
- 26 Colleen Sprigg; orcid.org/0000-0001-7755-4245
- 27 Hayley L. Whitfield; orcid.org/0000-0001-6003-7874

28

- 29 Figure S1. LC-ICP-MS analysis of InsP₆ digestion in the avian gastrointestinal tract.
- 30 Figure S2. Biological variability and reproducibility of LC-ICP-MS
- Table S1. Statistical analysis of phytase inclusion in diet on inositol phosphate content of gut tissues

- 32 Table S2. Analysis of effect of phytase inclusion in diet on InsP₅: InsP₆ ratio of gut tissues
- 33 Table S3. Inositol phosphate levels in duodenal segments of chicken
- Table S4. Inositol phosphate levels in jejunum segments of chicken
- 35 Table S5. Inositol phosphate levels in ileum segments of chicken
- 36 Table S6. Dietary treatments and Test Substance inclusion rates

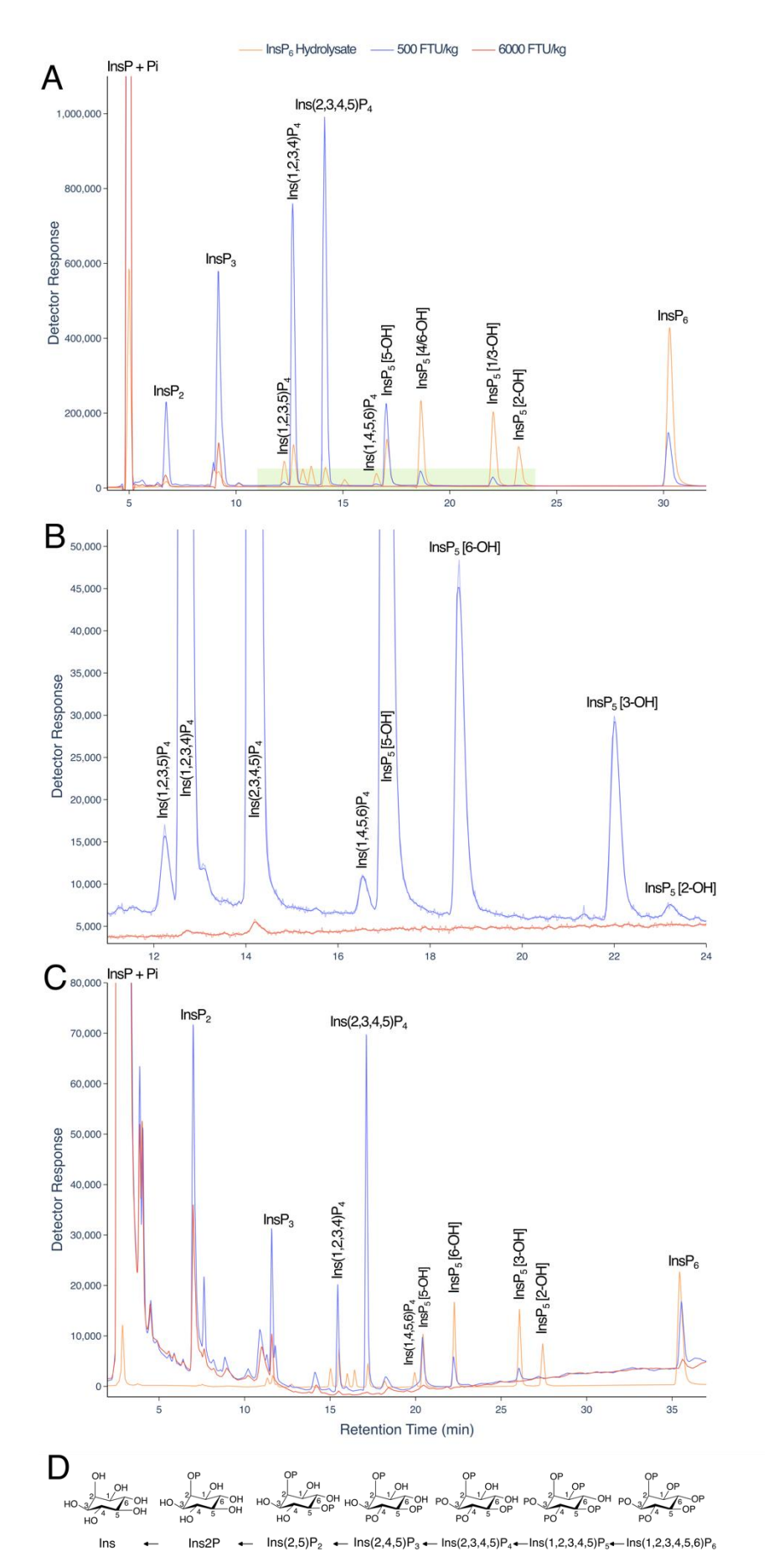
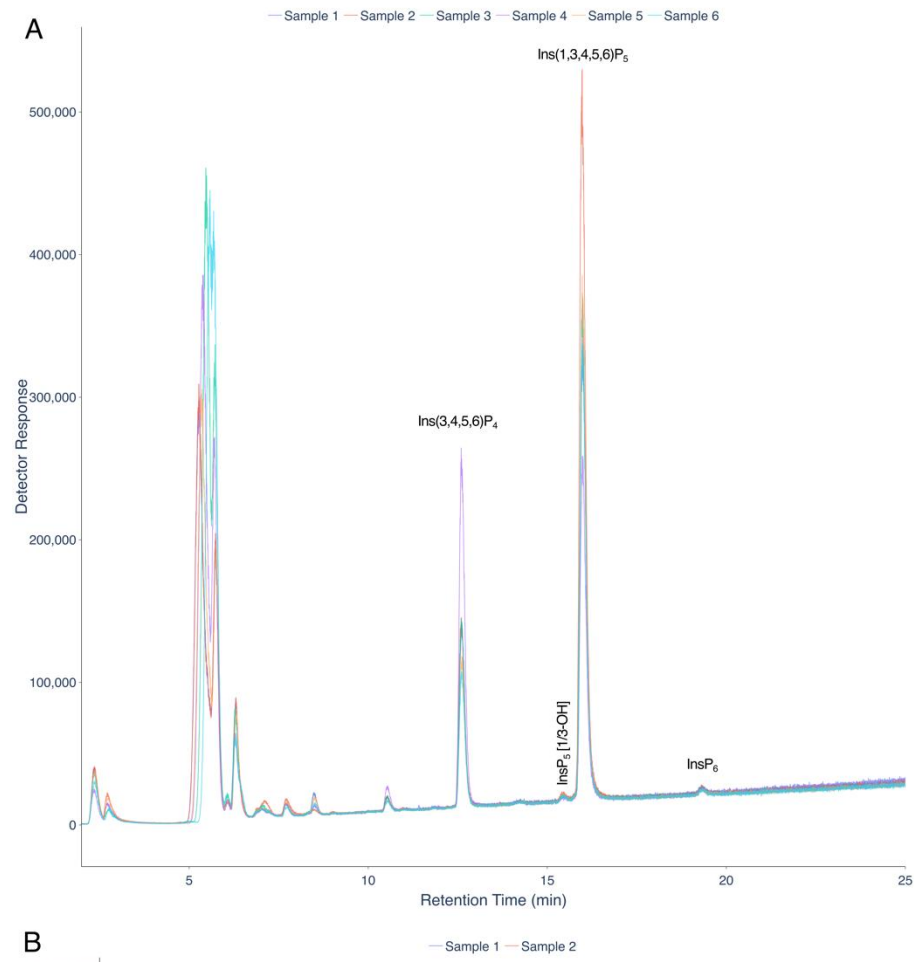


Figure S1. LC-ICP-MS analysis of InsP₆ digestion in the avian gastrointestinal tract. A. LC-ICP-MS of lumenal gizzard content of birds fed a diet containing low (500 FTU/kg) (blue) or high (6000 FTU/kg) (red) phytase, beside a hydrolysate of InsP₆ (orange). B. An expansion of the InsP₄ and InsP₅ region, indicated by the pale green panel, of the 500 FTU/kg and 6000 FTU/kg traces shown A. C. LC-UV analysis of lumenal content of gizzard of birds fed a diet containing low (500 FTU/kg) (blue) or high (6000 FTU/kg) (red) phytase, beside a hydrolysate of InsP₆ (orange). D. Pathway of degradation of InsP₆ by 6-phytase after ^{1,2,3}. Final digestive dephosphorylation of InsP is likely catalysed by alkaline phosphatase of the mucosal epithelia. For all panels, samples were resolved on a CarboPac PA200 column eluted with methanesulfonic acid. Separations of gut lumen inositol phosphates matching the resolution shown (A, B, C) have been observed on more than 1000 occasions at varying phytase dose on CarboPac PA200 coupled to LC-UV. For the ICP analysis shown, various digesta samples have been analysed on more than 10 occasions with equivalent resolution and detector response.



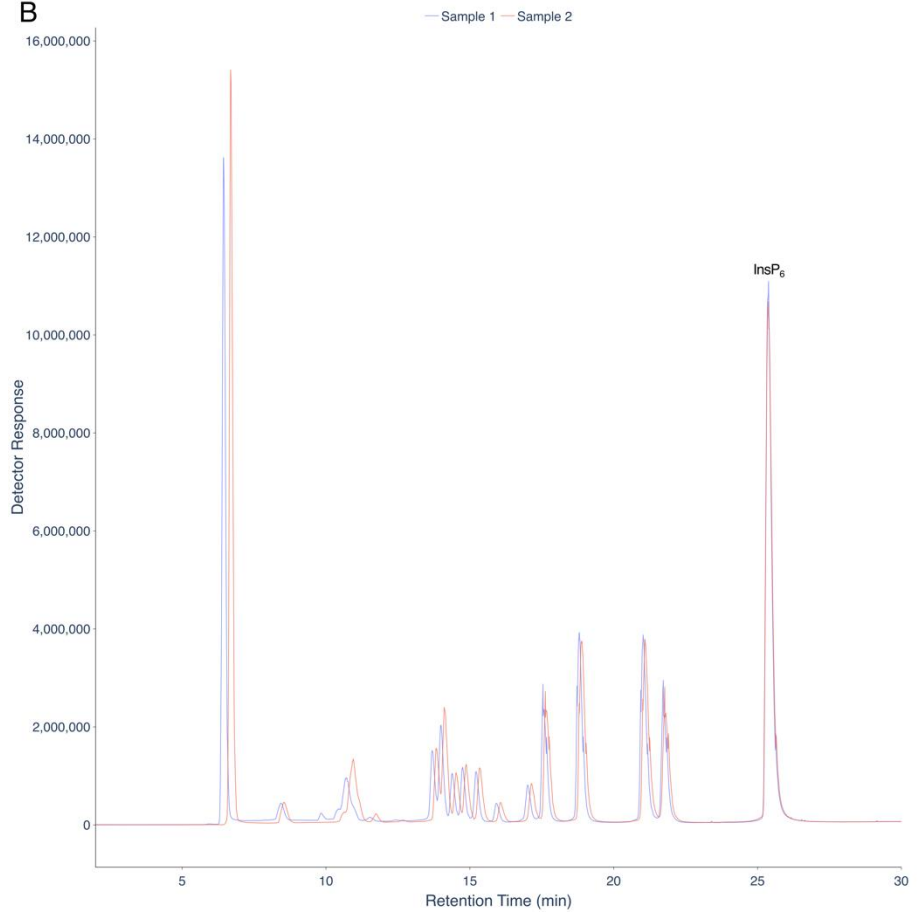


Figure S2. Biological variability and reproducibility of LC-ICP-MS. Inositol phosphate extracts were prepared from blood samples obtained from six 35 d old chickens raised in different pens and fed a control diet. Whole blood was extracted in $HClO_4$, diluted with NaF-EDTA and analysed by LC-ICP-MS. The samples were analysed at the end of a set of 25 consecutive injections. For $Ins(3,4,5,6)P_4$ and $Ins(1,3,4,5,6)P_5$, with mean retention time (and coefficient of variation) 12.06 min (0.070) and 15.987 min (0.011), the two peaks had areas with mean (and standard error) of 1,516,234 (244,855) and 4,191,724 (425,478), respectively. B) Two replicate injections of an $InsP_6$ hydrolysate sample were analysed at the end of a set of more than 50 consecutive injections. For these, the $InsP_6$ peak area (counts.min) were 161,430,343 and 171,113,2621. The $InsP_5$ peaks (not labelled), similarly, differed by less than 4% of the mean value for the duplicate measurements. In a separate experiment, three replicate injections of a different $InsP_6$ hydrolysate sample gave peak areas (counts.min) for $InsP_6$ of mean 2,041,016 and standard error 23,460. Different $InsP_6$ the $InsP_6$ of mean 2,041,016 and standard error 23,460. Different $InsP_6$ hydrolysate sample gave used for A and B.

Table S1. Analysis of effect of phytase inclusion in diet on inositol phosphate content of duodenum, jejunum and ileum tissue, analysed by a linear mixed-effects model with a log transformation (+1) applied to InsP measures. Phytase was added, or not, at 500 or 6000 FTU/kg. Inositol was added at 2g/kg.

log(value + 1)			
Predictors	Estimates (-	р
(Intercept)	0.43	0.24 – 0.62	<0.001
Control [Inositol_added]	0.42	0.18 - 0.66	0.001
Control [Phytase 500]	0.21	-0.03 – 0.45	0.092
Control [Phytase 6000]	0.29	0.05 – 0.53	0.019
InsP ₄	1.02	0.82 – 1.23	<0.001
InsP ₅	2.51	2.30 – 2.71	<0.001
InsP ₆	2.31	2.11 – 2.52	<0.001
Tissue [Jejunum]	0.25	0.06 - 0.44	0.011
Tissue [Ileum]	0.16	-0.03 – 0.35	0.098
Titanium [Yes]	0.11	0.00 - 0.22	0.041
Control [Inositol added] × InsP ₄	-0.47	-0.71 – -0.23	<0.001
Control [Phytase 500] × InsP ₄	0.05	-0.19 – 0.29	0.687
Control [Phytase 6000] × InsP₄	-0.21	-0.45 – 0.03	0.081
Control [Inositol added] × InsP ₅	-0.57	-0.81 – -0.34	<0.001
Control [Phytase 500] × InsP ₅	0.01	-0.22 – 0.25	0.918
Control [Phytase 6000] × InsP₅	-0.42	-0.65 – -0.18	0.001
Control [Inositol added] × InsP ₆	-0.71	-0.95 – -0.47	<0.001
Control [Phytase 500] × InsP ₆	-0.33	-0.56 – -0.09	0.007
Control [Phytase 6000] × InsP ₆	-1.10	-1.34 – -0.86	<0.001
InsP ₄ × Tissue [Jejunum]	-0.23	-0.43 – -0.02	0.031
InsP ₅ × Tissue [Jejunum]	-0.20	-0.41 - 0.00	0.054
InsP ₆ × Tissue [Jejunum]	-0.01	-0.22 – 0.19	0.899
InsP ₄ × Tissue [Ileum]	0.37	0.16 - 0.58	<0.001
InsP ₅ × Tissue [Ileum]	-0.14	-0.35 – 0.06	0.166
InsP ₆ × Tissue [Ileum]	-0.17	-0.37 – 0.04	0.113
Control [Inositol added] × Tissue [Jejunum]	-0.20	-0.41 - 0.00	0.054
Control [Phytase 500] × Tissue [Jejunum]	-0.36	-0.57 – -0.16	0.001
Control [Phytase 6000] × Tissue [Jejunum]	-0.32	-0.52 – -0.11	0.003
Control [Inositol added] × Tissue [Ileum]	-0.54	-0.74 – -0.33	<0.001
Control [Phytase 500] × Tissue [Ileum]	-0.25	-0.45 – -0.04	0.018
Control [Phytase 6000] × Tissue [Ileum]	-0.18	-0.39 – 0.03	0.086
Random Effects			
σ^2	0.26		
τ _{00 id}	0.05 0.16		
·	0.10		

Observations 1152
Marginal R² / Conditional R² 0.705 / 0.753

Table S2. Analysis of effect of phytase inclusion in diet on $InsP_5$: $InsP_6$ ratio of duodenum, jejunum and ileum tissue, analysed by a linear mixed-effects model with a square root transformation applied to ratios. Phytase was added, or not, at 500 or 6000 FTU/kg. Inositol was added at 2g/kg.

	s	sqrt(InsP ₅ : InsP ₆)	
Predictors	Estimates	CI	p
(Intercept)	1.28	1.10 – 1.47	<0.001
Control [Inositol added]	-0.01	-0.26 – 0.23	0.918
Control [Phytase 500]	0.17	-0.07 – 0.42	0.169
Control [Phytase 6000]	0.40	0.15 - 0.65	0.002
Tissue [Jejunum]	-0.21	-0.45 – 0.02	0.076
Tissue [lleum]	0.12	-0.12 – 0.35	0.335
Titanium [Yes]	-0.10	-0.22 – 0.01	0.062
Control [Inositol added] × Tissue [Jejunum]	0.24	-0.10 – 0.57	0.164
Control [Phytase 500] × Tissue [Jejunum]	0.14	-0.19 – 0.48	0.395
Control [Phytase 6000] × Tissue [Jejunum]	0.20	-0.13 – 0.53	0.240
Control [Inositol added] × Tissue [Ileum]	0.02	-0.31 – 0.36	0.897
Control [Phytase 500] × Tissue [Ileum]	-0.10	-0.44 – 0.23	0.541
Control [Phytase 6000] × Tissue [Ileum]	-0.10	-0.44 – 0.23	0.536
Random Effects			
σ^2	0.17		
₹00 id	0.02		
₹00 Diet	0.00		
N _{id}	96		
N _{Diet}	8		
Observations	286		-
Marginal R ² / Conditional R ²	0.173 / NA	A	

Table S3. Inositol phosphate levels (nmol/g wwt) in duodenal segments of day 21 broilers

Diet	InsP ₃	InsP ₄	InsP ₅	InsP ₆	∑InsP
Control	0.6±0.1 ^b	4.1±0.7	21.2±4.2	14.4±3.9	40.3±8.4
2g/kg inositol	1.1±0.2 ^{ab}	2.6±0.5	12.0±1.2	13.5±4.7	29.2±5.2
Phy500	0.8±0.1 ^{ab}	5.0±0.6	26.1±2.7	13.0±1.0	44.9±3.3
Phy6000	1.2±0.1 ^{ab}	5.8±0.5	26.7±2.2	9.2±0.9	42.9±3.1
Control TiO ₂	0.9±0.2 ^{ab}	4.6±0.5	24.1±2.6	22.7±4.2	52.2±3.6
2g/kg inositol TiO ₂	2.8±0.2 ^{aa}	4.0±0.5	21.7±2.3	21.1±6.7	49.7±8.1
Phy500 TiO ₂	1.1±0.2 ^{ab}	5.3±0.4	27.9±1.8	16.5±2.6	50.7±4.2
Phy6000 TiO ₂	1.1±0.2 ^{ab}	3.0±0.6	12.4±1.6	13.5±0.5	21.8±2.1

Data are given as group means \pm SEM, n=12 (6 pens per diet with samples from 2 broilers per pen per treatment). Statistical analysis was performed by multiple T-tests with correction for multiple comparisons using the Holm-Šidák method. Differences in superscripts within columns indicate differences, at p < 0.05, between groups.

Table S4. Inositol phosphate levels (nmol/g wwt) in jejunum segments of day 21 broilers

Diet	InsP ₃	InsP ₄	InsP ₅	InsP ₆	∑InsP
Control	1.2±0.1	3.8±0.6	19.5±2.3	33.5±8.9 ^a	58.0±9.8 ^a
2g/kg inositol	0.8±0.2	2.2±0.5	12.6±1.6	20.9±8.0 ^{ab}	36.4±8.2 ^{ab}
Phy500	1.4±0.3	4.1±0.4	22.3±3.2	11.4±2.5 ^b	39.2±4.6 ^{ab}
Phy6000	1.8±0.6	5.0 ±1.3	15.7±2.1	5.8±0.8 ^b	28.3±2.8 ^b
Control TiO ₂	1.2±0.2	3.8±0.6	22.6±3.1	29.7±6.0 ^{ab}	57.3±6.7 ^{ab}
2g/kg inositol TiO ₂	1.7±0.2	4.5±0.3	20.2±1.4	14.8±3.2 ^{ab}	41.2±3.8 ^{ab}
Phy500 TiO ₂	0.9±0.2	2.7±0.5	16.1±1.9	16.2±3.0 ^{ab}	25.9±4.2 ^{ab}
Phy6000 TiO ₂	1.0±0.2	2.6±0.7	14.0±2.7	6.1±1.1 ^{ab}	23.9±4.5 ^b

Data are given as group means \pm SEM, n=12 (6 pens per diet with samples from 2 broilers per pen per treatment). Statistical analysis was performed by multiple T-tests with correction for multiple comparisons using the Holm-Šidák method. Differences in superscripts within columns indicate differences, at p < 0.05, between groups.

Table S5. Inositol phosphate levels (nmol/g wwt) in ileum segments of day 21 broilers

Diet	InsP ₃	InsP ₄	InsP ₅	InsP ₆	∑InsP
Control	1.0±0.1	10.2±1.2 ^a	28.1±2.5 ^a	18.6±7.9	58.0±7.8 ^a
2g/kg inositol	0.4±0.2	2.2±5.6 b	5.6±2.7 ^b	3.3±0.8	11.5±2.7 ^b
Phy500	1.4±0.5	10.8±3.0 ^{ab}	21.2±2.1 ^a	11.5±2.4	45.0±6.6 ^{ab}
Phy6000	1.2±0.3	4.6±0.5 b	12.6±1.4 ^b	6.1±0.9	24.6±2.4 ^b
Control TiO ₂	0.8±0.1	5.4±0.9 ^{ab}	17.0±1.8 ^b	40.3±21.0	63.5±20.0 ^{ab}
2g/kg inositol TiO ₂	1.8±0.2	7.9±1.3 ^{ab}	19.1±2.7 ^b	18.3±6.7	47.1±7.3 ^{ab}
Phy500 TiO ₂	0.6±0.1	5.6±0.4 ^{ab}	17.3±1.7 ^b	21.4±8.5	44.9±8.9 ^{ab}
Phy6000 TiO ₂	1.4±0.3	8.3±1.4 ^{ab}	18.4±2.7 ^b	5.9±0.6	34.0±4.2 ^{ab}

Data are given as group means \pm SEM, n=12 (6 pens per diet with samples from 2 broilers per pen per treatment). Statistical analysis was performed by multiple T-tests with correction for multiple comparisons using the Holm-Šidák method. Differences in superscripts within columns indicate differences, at p < 0.05, between groups.

Table S6: Dietary treatments and Test Substance inclusion rates, after 4

Dietary Treatment	Test Substance inclusion rates to the basal diet				
	Phytase (g/tonne) ¹³ C Inositol mix (g/tonne)		TiO ₂ (g/tonne)		
Control	-	-	-		
2 g/kg Ins	-	2000	-		
Phy500	100	-	-		
Phy6000	1200	-	-		
Control TiO ₂	-	-	5000		
2 g/kg Ins TiO ₂	-	2000	5000		
Phy500 TiO ₂	100	-	5000		
Phy6000 TiO ₂	1200	-	5000		

References

- Sommerfeld, V., Kunzel, S., Schollenberger, M., Kuhn, I., Rodehutscord, M. Influence of phytase or *myo*-inositol supplements on performance and phytate degradation products in the crop, ileum, and blood of broiler chickens. *Poult Sci* **97**, 920-929 (2018). 10.3382/ps/pex390
- Sommerfeld, V., Schollenberger, M., Kuhn, I., Rodehutscord, M. Interactive effects of phosphorus, calcium, and phytase supplements on products of phytate degradation in the digestive tract of broiler chickens. *Poult Sci* **97**, 1177-1188 (2018). 10.3382/ps/pex404
- Greiner, R., Konietzny, U., Jany, K.D. Purification and characterization of two phytases from *Escherichia coli*. *Arch Biochem Biophys* **303**, 107-113 (1993). 10.1006/abbi.1993.1261
- 4 Sprigg, C., Leftwich, P.T., Burton, E., Scholey, D., Bedford, M.R., Brearley, C.A. Accentuating the positive and eliminating the negative: Efficacy of TiO₂ as digestibility index marker for poultry nutrition studies. *PLoS One* **18**, e0284724 (2023). 10.1371/journal.pone.0284724